Article

pubs.acs.org/Biomac

Synthesis of Poly[*N*-(2-hydroxypropyl)methacrylamide] Conjugates of Inhibitors of the ABC Transporter That Overcome Multidrug Resistance in Doxorubicin-Resistant P388 Cells in Vitro

V. Šubr,*[,†] L. Sivák,[‡] E. Koziolová,[†] A. Braunová,[†] M. Pechar,[†] J. Strohalm,[†] M. Kabešová,[‡] B. Říhová,[‡] K. Ulbrich,[†] and M. Kovář[‡]

[†]Institute of Macromolecular Chemistry, Academy of Sciences of the Czech Republic v.v.i., Heyrovsky Sq. 2, 162 06 Prague 6, Czech Republic

[‡]Institute of Microbiology, Academy of Sciences of the Czech Republic v.v.i., Vídeňská 1083, 142 20 Prague 4, Czech Republic

Supporting Information

ABSTRACT: The effects of novel polymeric therapeutics based on water-soluble *N*-(2-hydroxypropyl)methacrylamide copolymers (*P*(HPMA)) bearing the anticancer drug doxorubicin (Dox), an inhibitor of ABC transporters, or both, on the viability and the proliferation of the murine monocytic leukemia cell line P388 (parental cell line) and its doxorubicin-resistant subline P388/MDR were studied in vitro. The inhibitor derivatives 5-methyl-4-oxohexanoyl reversin 121 (MeOHe-R121) and 5-methyl-4-oxohexanoyl ritonavir ester (MeOHe-RIT), showing the highest inhibitory activities, were conjugated to the *P*(HPMA) via the biodegradable pH-sensitive hydrazone bond, and the ability of these conjugates to block the ATP driven P-glycoprotein (P-gp) efflux pump was tested. The *P*(HPMA) conjugate *P*-Ahx-NH-N═MeOHe-R121 showed a dose-dependent increase in the ability to sensitize the P388/MDR cells to Dox from 1.5 to 24 μM, and achieved an approximately 50-fold increase in sensitization at 24 μM. The *P*(HPMA) conjugate *P*-Ahx-NH-N═MeOHe-RIT showed moderate activity at 6 μM (~10 times higher sensitization) and increased sensitization by 50-fold at 12 μM. The cytostatic activity of the *P*(HPMA) conjugate *P*-Ahx-NH-N═MeOHe-R121(Dox) containing Dox and the P-gp inhibitor MeOHe-R121, both bound via hydrazone bonds to the *P*(HPMA) carrier, was almost 30 times higher than that of the conjugate *P*-Ahx-NH-N═Dox toward the P388/MDR cells in vitro. A similar result was observed for *P*-Ahx-NH-N═MeOHe-RIT(Dox), which exhibited almost 10 times higher cytostatic activity than *P*-Ahx-NH-N═Dox.

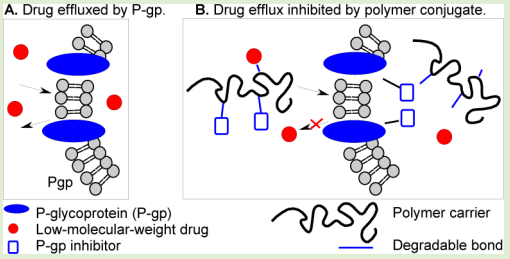

INTRODUCTION

One of the most serious problems for chemotherapy is the gradual development of resistance of the cancer cells, which are originally highly sensitive, to treatment with the wide spectrum of anticancer drugs commonly used in cancer chemotherapy. This phenomenon is called acquired multidrug resistance (MDR) and is the result of the overexpression of adenosine triphosphate-binding cassette proteins (ABC transporters) in tumor cells. MDR is responsible for a significant proportion of chemotherapy failure in cancer treatment.[1−5] The energy-dependent efflux of various hydrophobic anticancer drugs, such as anthracyclines, vinca alkaloids, taxanes, and others, by the ABC transporters reduces the intracellular concentration of the drugs below the effective cytotoxic threshold and is the major mechanism of MDR. In humans, 48 genes encoding ABC transporters have been classified. P-glycoprotein (P-gp), breast cancer resistance protein (BCRP), and multidrug resistance proteins (MRPs) are considered to be the most important of these genes.[4,6]

Inhibition of the ABC transporters by low-molecular-weight inhibitors seems to be one of the most promising approaches for overcoming MDR in cancer cells. Three generations of inhibitors of ABC transporters have been described. Third generation inhibitors, including elacridar, zosuquidar, and tariquidar, effectively block the efflux function of the ABC transporters at nanomolar concentrations.[2,4,7,8]

In addition to these molecules, a series of short peptide P-gp inhibitors called reversins have been synthesized and described. They consist of di- and tripeptide derivatives that share common physicochemical and structural features, such as bulky aromatic and/or alkyl groups. Reversin 121 (Boc-Asp(OBzl)-Lys(Z)-OtBu) is an aspartyl lysine (Asp-Lys) dipeptide derivative, and reversin 205 (N^{α},N^{ε}-bis[Boc-Glu(OBzl)-Lys-OMe) is a tripeptide derivative with a high inhibitory activity for P-gp.[9] The potentials of reversin 121 and reversin 205 have been studied in MDR1-expressing tumor cells in vitro,[10,11] and reversin 121 has been studied in a murine pancreatic tumor cell line Panc02 in vivo.[12]

Several analogues of reversin 121 and reversin 213 were synthesized to evaluate their ability to inhibit P-gp-mediated

Received: May 5, 2014
Revised: June 25, 2014

   dx.doi.org/10.1021/bm500649q | *Biomacromolecules* XXXX, XXX, XXX−XXX

Table 1. Physicochemical Characteristics of the Inhibitor Derivatives

inhibitor derivative	mp [°C]	ESI-MS m/z $(M - Na)^+$	elemental analysis, calcd/found			
			C	H	N	S
reversin 121	87−88	664.1	63.83/64.16	7.09/7.80	6.57/6.79	
OPe-R121	57−58	662.33	63.83/63.53	7.09/6.9	6.57/6.56	
OHe-R121	70−71	690.33	64.75/64.68	7.40/7.36	6.29/6.31	
MeOHe-R121	62−64	690.33	64.75/65.03	7.40/7.27	6.29/6.18	
OPB-R121	73−74	724.17	66.74/66.51	6.75/6.67	5.99/5.92	
Ma-Ahx-R121	54−56	745.17	64.8/64.68	7.53/7.88	7.75/7.58	
OHe-RIT	49−51	869.42	62.39/61.81	6.90/7.48	9.92/9.66	7.57/7.58
MeOHe-RIT	52−54	869.17	62.39/62.00	6.90/6.87	9.92/9.60	7.57/7.12
OPe-RIT	n.d.[a]	841.58	62.69/62.12	6.80/7.34	10.07/10.31	7.44/7.22
OPB-RIT	n.d.	903.50	64.07/63.53	6.41/6.59	9.54/9.33	7.28/7.44
Ma-Ahx-RIT	51−53	902.41	62.57/61.63	7.04/7.63	10.87/10.04	7.11/6.81
MeOHe-R205	109−112	847.50	n.d.	n.d.	n.d.	n.d.

[a]n.d. = not determined.

drug efflux in NIH3T3 mouse cells or K562/R7 human erythroleukemic cells, which overexpress P-gp. These analogues retained good activity compared to cyclosporin A and the original reversins.[13,14]

Omelyanenko et al.[15] have hypothesized that the administration of anticancer drugs as water-soluble polymeric conjugates will be inaccessible to the energy-driven P-gp-mediated efflux pump, thus increasing the intracellular drug concentration in P-gp-expressing MDR cells when compared to the free drug.

Polymer-bound drugs,[16,17] micelles,[18−20] liposomes,[21,22] and nanoparticles[23−25] are internalized by endocytosis through endosomes/lysosomes and ultimately accumulate inside the cell. Thus, these forms of drugs should be inaccessible to the energy-dependent efflux pump localized at the cytoplasmic membrane.

The results obtained by Minko et al. indicate that water-soluble anticancer drug conjugates based on a *N*-(2-hydroxypropyl)methacrylamide copolymer *P*(HPMA) containing doxorubicin (Dox) bound via the lysosomally degradable GlyPheLeuGly spacer are partially able to avoid the P-gp-mediated efflux of Dox in the Dox-resistant A2780/AD human ovarian carcinoma cell line.[26−29]

Zhao et al. described the synthesis of liposomes loaded with epirubicin and their biological activity in MDA-MB 435 cells and their MDR counterparts (MDA-MB 435/ADR) in vitro. They also described a tumor growth inhibition model in vivo. Epirubicin-loaded liposomes effectively inhibited growth in both cell lines.[22]

Hydrolytically degradable hydrogels based on *N*-(2-hydroxypropyl)methacrylamide (HPMA) loaded with Dox and cyclosporin A were also used in combined therapy against the mouse P388/MDR leukemia, and a synergistic effect of the cytostatic drug and the chemosensitizing agent was observed. The tumor volumes were reduced to approximately 50% after the implantation of a HPMA hydrogel containing four times the maximum tolerated dose (MTD) of Dox and cyclosporine A (CsA).[30]

Pluronic P85 block copolymers loaded with daunorubicin were studied in the P-gp-overexpressing human ovarian carcinoma cells, SKVLB, and non-MDR SKOV3 cells. A dramatic increase in the daunorubicin cytotoxic activity (up to 700 times) was observed in the presence of 0.01%−1% copolymer in the case of the SKVLB cells.[18,19,31]

The aim of this study was to investigate the potential of novel polymeric therapeutics based on water-soluble *P*(HPMA) copolymers bearing either an anticancer drug, an inhibitor of ABC transporters or both. Binding of the anticancer drug or an inhibitor of the ABC transporters to the polymeric carrier should significantly prolong their blood circulation, improve their solubility and overcome nonspecific side effects on healthy tissue due to passive accumulation in solid tumors via the enhanced permeability and retention (EPR) effect.[32] The P-gp inhibitor in the conjugate will further increase the intracellular load of the cancerostatic drug in MDR cancer cells. Here, we tested the inhibitory activity of low-molecular-weight derivatives of reversin 121, reversin 205 (N^{α}, N^{ε}-bis[Boc-Glu(OBzl)-Lys-OMe), and ritonavir and the *P*(HPMA) conjugates containing these derivatives, bound via a biodegradable pH-sensitive hydrazone bond, in the Dox-resistant P388/MDR mouse leukemia and the sensitive parental P388 cell lines.

MATERIALS AND METHODS

Materials. Methacryloyl chloride, 1-amino-propan-2-ol, 2,2′-azobis-(2-methylbutyronitrile) (AIBN), 4,5-dihydro-thiazole-2-thiol (TT), Boc-hydrazide, 2-cyanopropan-2-yl benzodithioate (CTA), 4-oxo-pentanoic acid, 6-oxo-heptanoic acid, succinic anhydride, iron(III) acetylacetonate, isopropylmagnesium chloride (2 M solution in THF), 4-(dimethylamino)pyridine (DMAP, *N*-ethyl-*N*′-(3-(dimethylamino)-propyl)carbodiimide hydrochloride (EDC), *N*,*N*′-dicyclohexyl carbodiimide (DCC), (benzotriazol-1-yloxy)tripyrrolidinophosphonium hexafluorophosphate (PYBOP), 1-hydroxybenzotriazole hydrate (HOBT), 2,4,6-trinitrobenzenesulfonic acid (TNBSA), *N*,*N*-diisopropylethylamine (DIPEA), triethylamine (Et_3N), *N*,*N*-dimethylformamide (DMF), dimethyl sulfoxide (DMSO), *tert*-butyl alcohol (*t*-BuOH), dichloromethane (DCM), and silica gel 60 were purchased from Sigma-Aldrich, Czech Republic. *N*-α-t-Boc-L-aspartic acid β-benzyl ester (Boc-Asp(OBzl)-OH), L-aspartic acid β-benzyl ester (H-Asp(OBzl)-OH), *N*-ε-CBZ-L-lysine *t*-butyl ester hydrochloride (H-Lys(Z)-OtBu·HCl), 4-Fmoc-hydrazinobenzoyl AM Nova Gel, Fmoc-Lys(ivDde)-OH, and Fmoc-Glu(OBz)-OH were purchased from Novabiochem. 4-(2-Oxopropyl)-benzoic acid was purchased from Rieke Metals Inc.. Ritonavir was purchased from ChemPacific Corp. Doxorubicin hydrochloride (Dox·HCl) was purchased from Meiji Seiko, Japan.

All other chemicals and solvents were of analytical grade. The solvents were dried and purified using conventional procedures and distilled before use.

Synthesis of Monomers. *N*-(2-Hydroxypropyl)methacrylamide (HPMA) was synthesized via the reaction of methacryloyl chloride

dx.doi.org/10.1021/bm500649q | Biomacromolecules XXXX, XXX, XXX−XXX

with 1-aminopropan-2-ol in dichloromethane in the presence of sodium carbonate.[33]

6-(2-Methyl-acryloylamino)-hexanoic acid (Ma-Ahx-COOH) was prepared as previously described.[34]

2-Methyl-*N*-[6-oxo-6-(2-thioxo-thiazolidin-3-yl)-hexyl]-acrylamide (Ma-Ahx-TT) was prepared as previously described.[35]

N′-[6-(2-Methyl-acryloylamino)-hexanoyl]-hydrazinecarboxylic acid *tert*-butyl ester (Ma-Ahx-NH-NH-Boc) was prepared by reaction of Ma-Ahx-COOH (3.0 g, 15.1 mmol) with Boc-hydrazide (2.09 g, 15.80 mmol) in the presence of EDC (3.75 g, 19.58 mmol) in DCM (20 mL). The reaction mixture was stirred for 3 h at room temperature and then extracted with distilled water (3 × 20 mL) and with an aqueous solution of $NaHCO_3$ (2 wt %). The organic layer was separated and dried over Na_2SO_4. The DCM was evaporated, and the product was crystallized from ethyl acetate. Yield: 2.13 g (45.2%). HPLC analysis showed a single peak at 220 nm with a retention time of 8.05 min., mp =139 °C. Elemental analysis: calcd/found C = 57.49/57.34%; H = 8.68/8.86%; N = 13.41/13.06%. ESI-MS: m/z = 335.96 $(M - Na)^+$.

Synthesis of the Inhibitor Reversin 121 and Derivatives of Reversin 121. *Synthesis of Boc-Asp(OBzl)-Lys(Z)-OtBu (Reversin 121).* Reversin 121 was prepared by the reaction of Boc-Asp(OBzl)-OH and H-Lys(Z)-OtBu·HCl as described earlier.[9] Boc-Asp(OBzl)-OH (0.1 g, 0.31 mmol), H-Lys(Z)-OtBu·HCl (0.115 g, 0.31 mmol), HOBT (0.044 g, 0.32 mmol), and Et_3N (45 μL, 0.32 mmol) were dissolved in DMF (5 mL), and the solution was cooled to −10 °C. DCC (0.07 g, 0.34 mmol) was dissolved in DMF (5 mL), and after cooling to −10 °C the two solutions were mixed. The reaction mixture was left overnight at 5 °C. The DMF was evaporated, and the solid residue was dissolved in ethyl acetate. The precipitated dicyclohexyl urea was removed by filtration, and the solution was extracted with an aqueous solution of citric acid (10% w/v) followed by extraction with a saturated solution of $NaHCO_3$. After drying the ethyl acetate phase over Na_2SO_4, the reversin 121 was crystallized from the ethyl acetate:hexane mixture. HPLC analysis gave a single peak at 220 nm with a retention time of 10.93 min. The other characteristics, including melting point, elemental analysis, and ESI-MS, are summarized in Table 1. The ^1H NMR spectra (300 MHz, DMSO, 296 K) are provided in the Supporting Information.

Synthesis of 1-(2-Thioxo-thiazolidin-3-yl)-pentane-1,4-dione (OPe-TT). 4-Oxo-pentanoic acid (2.0 g, 17.2 mmol) and 4,5 dihydro-thiazole-2-thiol (2.05 g, 17.2 mmol) were dissolved in DCM, and *N*-ethyl-*N*′-(3-(dimethylamino)propyl)carbodiimide hydrochloride (EDC) (3.95 g, 20.6 mmol) was added. The reaction mixture was stirred for 3 h at room temperature and then extracted with distilled water (3 × 20 mL) and with an aqueous solution of $NaHCO_3$ (2 wt %). The organic layer was separated and dried over Na_2SO_4. The DCM was evaporated, and the product was crystallized from ethyl acetate. Yield: 1.8 g (49%). HPLC analysis showed a single peak at 305 nm with a retention time of 8.55 min., mp = 82 °C. Elemental analysis: calcd/found C = 44.22/44.34%; H = 5.10/5.23%; N = 6.45/6.47%; S = 29.51/28.52%. ESI-MS: m/z = 239.92 $(M - Na)^+$.

The procedure described for the synthesis of OPe-TT was used for the synthesis of 1-(2-thioxo-thiazolidin-3-yl)-heptane-1,6-dione (OHe-TT), 5-methyl-1-(2-thioxo-thiazolidin-3-yl)-hexane-1,4-dione (MeOHe-TT), and 1-[4-(2-thioxo-thiazolidine-3-carbonyl)-phenyl]-propan-2-one (OPB-TT).

Synthesis of 1-(2-Thioxo-thiazolidin-3-yl)-heptane-1,6-dione (OHe-TT). The OHe-TT was prepared by the reaction of 6-oxohexanoic acid (1.03 g, 7.14 mmol) with 4,5 dihydro-thiazole-2-thiol (0.85 g, 7.14 mmol) in the presence of EDC (1.64 g, 8.57 mmol). Yield: 1.4 g (37%). HPLC analysis showed a single peak at 305 nm with a retention time of 9.12 min. Elemental analysis: calcd/found C = 48.95/49.01%; H = 6.16/6.14%; N = 5.71/5.66%; S = 26.14/25.84%. ESI-MS: m/z = 268.00 $(M - Na)^+$.

Synthesis of 5-Methyl-1-(2-thioxo-thiazolidin-3-yl)-hexane-1,4-dione (MeOHe-TT). 5-Methyl-4-oxohexanoic acid was synthesized according Barberis and Pérez-Prieto.[36] The MeOHe-TT was prepared by the reaction of 5-methyl-4-oxohexanoic acid (0.52 g; 3.58 mmol) with 4,5 dihydro-thiazole-2-thiol (0.43 g, 3.58 mmol) in the presence of EDC (0.82 g; 4.30 mmol). The yield was 1.4 g (37%) of an oily product, which was used in the next step without purification.

Synthesis of 1-[4-(2-Thioxo-thiazolidine-3-carbonyl)-phenyl]-propan-2-one (OPB-TT). The OPB-TT was prepared by the reaction of 4-(2-oxopropyl)-benzoic acid (1.02 g 5.74 mmol) with 4,5 dihydro-thiazole-2-thiol (0.69 g, 5.74 mmol) in the presence of EDC (1.43 g, 7.47 mmol). HPLC analysis showed a single peak at 305 nm with a retention time of 9.12 min., mp = 143−146 °C. Elemental analysis: calcd/found C = 55.89/54.43%; H = 4.69/4.24%; N = 5.01/5.29%; S = 22.96/22.80%. ESI-MS: m/z = 302.0 $(M - Na)^+$.

The ^1H NMR spectra (300 MHz, DMSO, 296 K) of OPe-TT, OHe-TT, and OPB-TT are provided in the Supporting Information.

Synthesis of OPe-Asp(OBzl)-Lys(Z)-OtBu (OPe-R121). H-Asp-(OBzl)-OH (0.5 g, 2.24 mmol) and $NaHCO_3$ (0.19 g, 2.24 mmol) were dissolved in a mixture of THF (10 mL) and distilled water (5 mL), and OPe-TT (0.49 g, 2.24 mmol) was then added. The reaction was carried out at room temperature for 24 h. The THF was evaporated, and the water phase was extracted with ethyl acetate (3 × 20 mL). The reaction mixture was acidified with HCl to pH = 2 and extracted with ethyl acetate (3 × 20 mL). The organic phase was dried over Na_2SO_4, and the ethyl acetate was evaporated. OPe-Asp(OBzl)-COOH was obtained as oily product (0.725 g) and was used in the next step without purification.

OPe-Asp(OBzl)-COOH (0.725 g, 2.24 mmol), H-Lys(Z)-Ot-Bu.HCl (0.93 g, 2.48 mmol), HOBT (0.34 g, 2.48 mmol), and DIPEA (0.42 mL, 2.24 mmol) were dissolved in DMF (5 mL), and EDC (0.57 g, 0.30 mmol) was then added. The reaction mixture was stirred for 24 h at room temperature. The DMF was evaporated, and the residue was dissolved in DCM and extracted with a 2 wt % aqueous solution of $KHSO_4$, $NaHCO_3$, and distilled water. The organic phase was dried over Na_2SO_4, and the solvent was evaporated. The oily crude product was dissolved in a 60:40 mixture of acetonitrile/distilled water, and the pure product was obtained by preparative HPLC on a Biospher PSI 120 C18 250 × 25 mm (Watrex) column with UV detection at 220 nm using the mobile phase water/acetonitrile with an acetonitrile gradient from 50% to 100%. The flow rate was 5 mL/min. The fractions with the pure product were collected and evaporated under vacuum. OPe-R121 was recrystallized from an ethyl acetate/hexane mixture. HPLC analysis showed a single peak at 220 nm with a retention time of 10.18 min. The other characteristics, including melting point, elemental analysis, and ESI-MS, are summarized in Table 1. The ^1H NMR spectra (300 MHz, DMSO, 296 K) are provided in the Supporting Information.

The procedure described above for the synthesis of OPe-R121 was used for the synthesis of OHe-Asp(OBzl)-Lys(Z)-OtBu (OHe-R121), MeOHe-Asp(OBzl)-Lys(Z)-OtBu (MeOHe-R121), OPB-Asp(OBzl)-Lys(Z)-OtBu (OPB-R121), and 6-(2-methyl-acryloylamino)-hexanoyl-Asp(OBzl)-Lys(Z)-OtBu (Ma-Ahx-R121).

Synthesis of OHe-Asp(OBzl)-Lys(Z)-OtBu (OHe-R121). OHe-Asp-(OBzl)-COOH was prepared by the reaction of H-Asp(OBzl)-OH (0.32 g, 1.44 mmol) with OHe-TT (0.32 g, 1.44 mmol) in the presence of $NaHCO_3$ (0.12 g, 1.44 mmol). In the next step, OHe-Asp(OBzl)-COOH (0.5 g, 1.44 mmol) was reacted with H-Lys(Z)-OtBu·HCl (0.59 g, 1.59 mmol), HOBT (0.21 g, 1.59 mmol), DIPEA (0.28 mL, 1.59 mmol), and EDC (0.37 g 1.91 mmol). HPLC analysis showed a single peak at 220 nm with a retention time of 10.27 min.

Synthesis of MeOHe-Asp(OBzl)-Lys(Z)-OtBu (MeOHe-R121). MeOHe-Asp(OBzl)-COOH was prepared by the reaction of H-Asp(OBzl)-OH (0.5 g, 2.24 mmol) with MeOHe-TT (0.55 g, 2.24 mmol) in the presence of $NaHCO_3$ (0.19 g, 2.24 mmol). In the next step, MeOHe-Asp(OBzl)-COOH (0.78 g, 2.24 mmol) was reacted with H-Lys(Z)-OtBu·HCl (0.92 g, 2.46 mmol), HOBT (0.33 g, 2.46 mmol), DIPEA (0.43 mL, 2.46 mmol), and EDC (0.52 g, 2.71 mmol). The yield was 1.129 g (75.5%). HPLC analysis showed a single peak at 220 nm with a retention time of 10.58 min.

Synthesis of OPB-Asp(OBzl)-Lys(Z)-OtBu (OPB-R121). OPB-Asp-(OBzl)-COOH was prepared by reaction of H-Asp(OBzl)-OH (0.6 g, 2.69 mmol) with OPB-TT (0.75 g, 2.69 mmol) in the presence of $NaHCO_3$ (0.23 g, 2.69 mmol). In the next step, OPB-Asp(OBzl)-COOH (1.02 g, 2.66 mmol) was reacted with H-Lys(Z)-OtBu·HCl

dx.doi.org/10.1021/bm500649q | *Biomacromolecules* XXXX, XXX, XXX−XXX

Scheme 1. Synthesis of Derivatives of Reversin 121

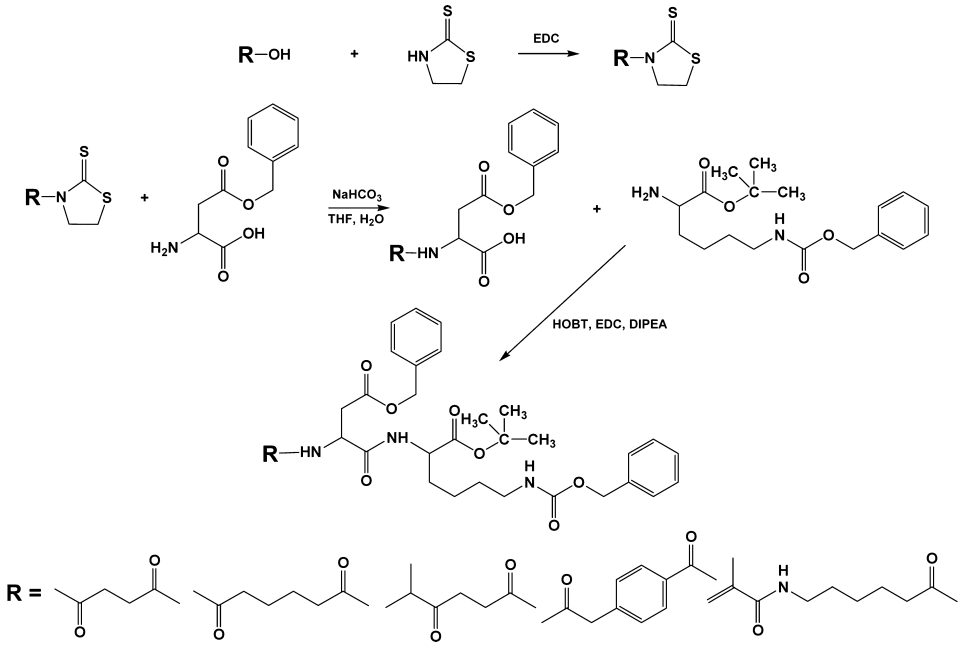

Scheme 2. Synthesis of Derivatives of Ritonavir

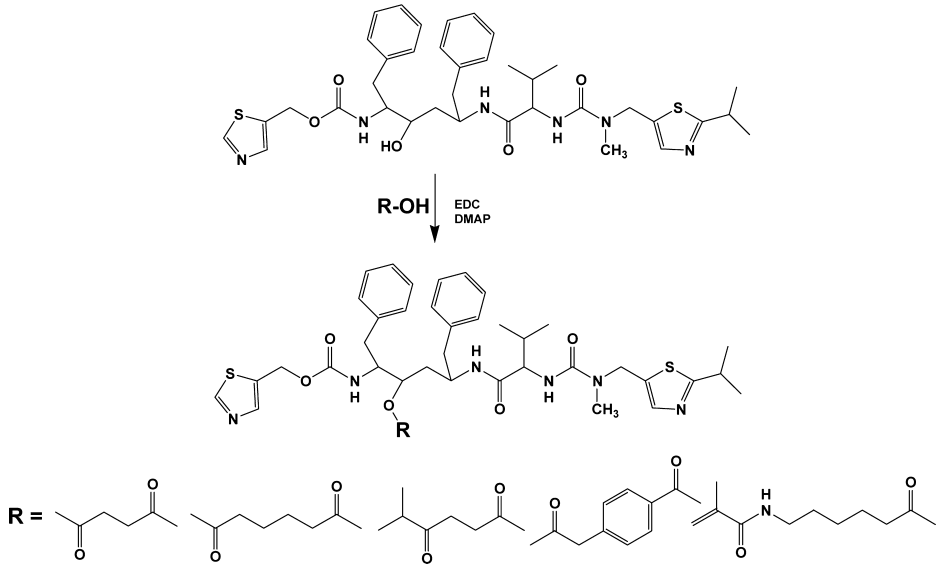

(0.99 g, 2.66 mmol), HOBT (0.36 g, 2.66 mmol), DIPEA (0.46 mL, 2.66 mmol), and EDC (0.66 g, 3.46 mmol). The crude product was purified on a silica gel column with a mobile phase of acetone/ethyl acetate/hexane (1:1:1) and crystallized from a mixture of diethyl ether/petrolether. The yield was 1.31 g (70.1%). HPLC analysis showed a single peak at 220 nm with a retention time of 10.46 min.

Synthesis of 6-(2-Methyl-acryloylamino)-hexanoyl-Asp(OBzl)-Lys(Z)-OtBu (Ma-Ahx-R121). Ma-Ahx-Asp(OBzl)-COOH was prepared by reaction of H-Asp(OBzl)-OH (0.36 g, 1.63 mmol) with Ma-Ahx-TT (0.49 g, 1.63 mmol) in the presence of $NaHCO_3$ (0.14 g, 1.63 mmol). In the next step, Ma-Ahx-Asp(OBzl)-COOH (0.65 g, 1.61 mmol) was reacted with H-Lys(Z)-OtBu.HCl (0.60 g, 1.61 mmol), HOBT (0.22 g, 1.61 mmol), DIPEA (0.28 mL, 1.61 mmol), and EDC (0.46 g, 2.41 mmol). Ma-Ahx-R121 was isolated from the reaction mixture by gel filtration on a silica gel column using a mobile phase of ethyl acetate/methanol 90:10 (v/v) and crystallized from a mixture of ethyl acetate/diethyl ether. The yield was 0.78 g (66.8%). The HPLC analysis gave a single peak at 220 nm with a retention time of 9.67 min.

The synthetic scheme of the reversin 121 derivatives is shown in Scheme 1, and the other characteristics, including melting point, elemental analysis, and ESI-MS, of OPe-R121, OHe-R121, MeOHe-R121, OPB-R121, and Ma-Ahx-R121 are summarized in Table 1. The ^1H NMR spectra (300 MHz, DMSO, 296 K) are provided in the Supporting Information.

Synthesis of 6-Oxoheptanoyl-ritonavir Ester (OHe-RIT). OHe-RIT was prepared by esterification of ritonavir with 6-oxoheptanoic acid. Ritonavir (0.1 g, 0.14 mmol) and 6-oxoheptanoic acid (0.026 g, 0.18 mmol) were dissolved in DCM (2 mL), and EDC (0.053 g, 0.276 mmol) was added. The reaction was catalyzed by DMAP. The reaction mixture was stirred at room temperature for 20 h and then extracted with distilled water (3 × 5 mL) and an aqueous solution of $NaHCO_3$ (2 wt %). The organic layer was separated and dried over Na_2SO_4, and the DCM was evaporated under reduced pressure. The oily crude product was dissolved in a 60:40 mixture of acetonitrile/distilled water, and the pure product was obtained by HPLC on a semipreparative column (Chromolith SemiPrep Rp18e 100 × 10 mm) with UV

dx.doi.org/10.1021/bm500649q | *Biomacromolecules* XXXX, XXX, XXX−XXX

Scheme 3. Synthesis of MeOHe-R205

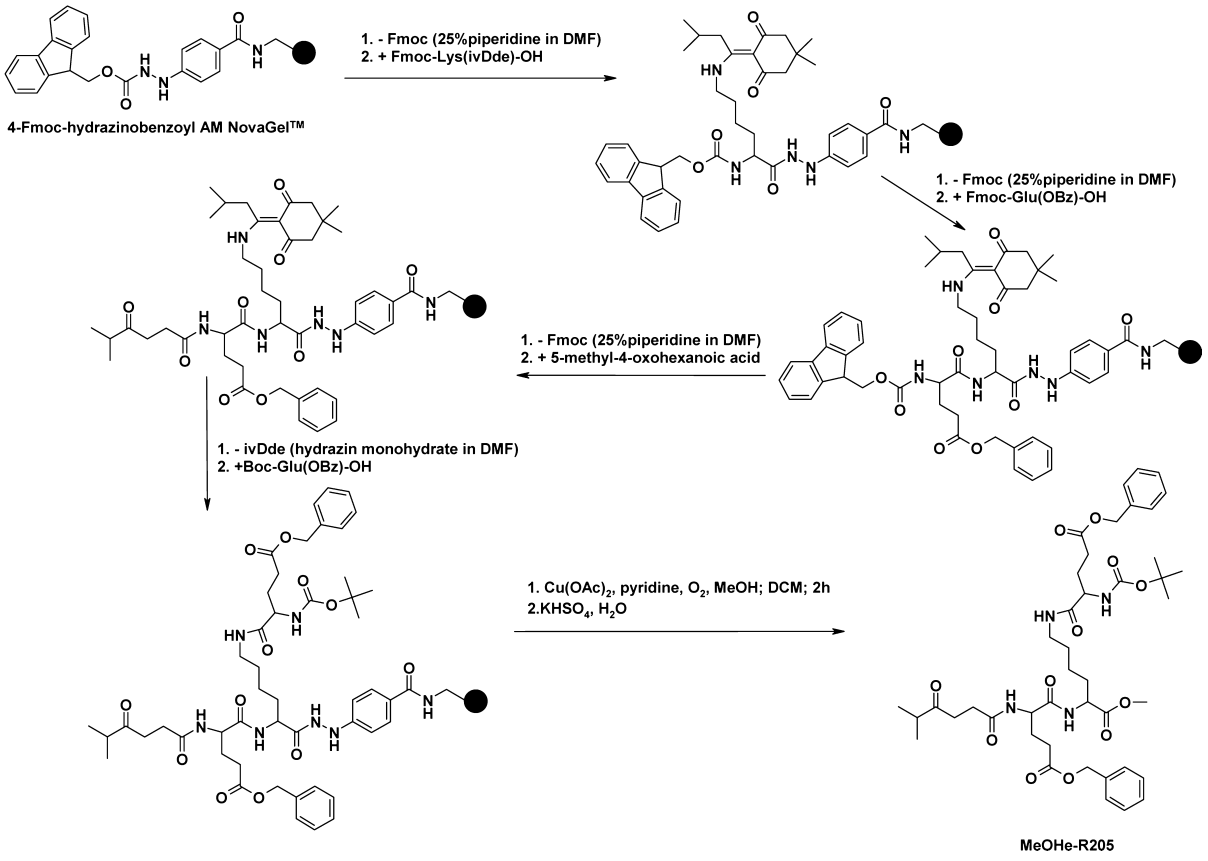

detection at 236 nm. The fraction containing the pure product was collected and evaporated under reduced pressure to dryness. The yield was 0.055 g (47%). The HPLC analysis showed a single peak at 236 nm with a retention time of 9.81 min.

The synthetic scheme for the ritonavir esters is shown in Scheme 2, and the other characteristics, including melting point, elemental analysis, and ESI-MS, for all synthesized ritonavir esters (OPe-RIT, OHe-RIT, MeOHe-RIT, OPB-RIT, and Ma-Ahx-RIT) are summarized in Table 1. The ^{1}H NMR spectra (300 MHz, MeOH, 296 K) are provided in the Supporting Information.

The procedure for the OHe-RIT synthesis described above was also used for the synthesis of the other ritonavir esters, that is, 5-methyl-4-oxohexanoyl-ritonavir ester (MeOHe-RIT), 5-oxohexanoyl-ritonavir ester (OHe-RIT), 4-oxopentanoyl-ritonavir ester (OPe-RIT), 4-(2-oxo-propyl)-benzoyl-ritonavir ester (OPB-RIT), and 6-(2-methyl-acryloylamino)-hexanoyl-ritonavir ester (Ma-Ahx-RIT).

Synthesis of 5-Methyl-4-oxohexanoyl-ritonavir Ester (MeOHe-RIT). MeOHe-RIT was prepared by esterification of ritonavir with 5-methyl-4-oxohexanoic acid, catalyzed by DMAP. Ritonavir (0.1 g, 0.139 mmol), DMAP, and 5-methyl-4-oxohexanoic acid (0.026 g, 0.18 mmol) were dissolved in DCM (2 mL), and EDC (0.053 g, 0.276 mmol) was added. The reaction mixture was stirred at room temperature for 5 h and then extracted with distilled water (3 × 5 mL) and an aqueous solution of $NaHCO_3$ (2 wt %). The organic layer was separated and dried over Na_2SO_4. The pure product was obtained by chromatography on a silica gel column (mobile phase chloroform/ethyl acetate/acetone 5:2:5) with UV detection at 236 nm. HPLC analysis showed a single peak at 236 nm with a retention time of 10.78 min. The yield was 0.095 g (82%).

Synthesis of 4-(2-Oxopropyl)-benzoyl-ritonavir Ester (OPB-RIT). OPB-RIT was prepared by esterification of ritonavir (0.15 g, 0.208 mmol) with 4-(2-oxopropyl)-benzoic acid (0.048 g, 0.27 mmol) in the presence of EDC (0.080 g, 0.416 mmol), catalyzed by DMAP, using the procedure described for MeOHe-RIT. The pure product was obtained as described for OHe-RIT. The yield was 0.117 g (64%). HPLC analysis showed a single peak at 236 nm with a retention time of 12.25 min.

Synthesis of 4-Oxopentanoyl-ritonavir Ester (OPe-RIT). OPe-RIT was prepared by esterification of ritonavir (0.15 g, 0.208 mmol) with 4-oxopentanoic acid (0.029 g, 0.25 mmol) using EDC (0.080 g, 0.416 mmol). The reaction was catalyzed by DMAP. The pure product was obtained using the same method as described for OHe-RIT and OPB-RIT. The yield was 0.12 g (70%). HPLC analysis showed a single peak at 236 nm with a retention time of 9.25 min.

Synthesis of 6-(2-Methyl-acryloylamino)-hexanoyl-ritonavir Ester (Ma-Ahx-RIT). Ma-Ahx-RIT was prepared by esterification of ritonavir (0.2 g, 0.28 mmol) with Ma-Ahx-COOH (0.072 g, 0.36 mmol) using EDC (0.106 g, 0.56 mmol) in DCM (4 mL). The reaction was catalyzed by DMAP, and the reaction mixture was stirred at room temperature overnight. The reaction mixture was extracted with distilled water (3 × 5 mL) and an aqueous $NaHCO_3$ solution (2 wt %). The organic layer was separated, dried over Na_2SO_4, and evaporated under vacuum. MA-Ahx-RIT was obtained by trituration of the residue with hexane. The yield was 0.12 g (48%). HPLC analysis showed a single peak at 236 nm with a retention time of 10.55 min.

Synthesis of [N^{α}-MeOHe-Glu(OBzl), N^{ε}-Boc-Glu(OBzl)]-Lys-OMe (MeOHe-R205). The protected tripeptide was synthesized (Scheme 3) through manual solid phase peptide synthesis, starting from the C-terminus, using a standard Fmoc strategy with 4-Fmoc-hydrazino-benzoyl AM Nova Gel (1.02 g; 0.56 mmol/g), PyBOP (3 equiv), HOBt monohydrate (3 equiv), and DIPEA (6 equiv) in DMF. The product was assembled by consecutive condensations of Fmoc-Lys(ivDde)-OH (3 equiv), Fmoc-Glu(OBz)-OH (3 equiv), and 5-methyl-4-oxohexanoic acid (3 equiv). After each condensation step, the Fmoc protecting groups were removed using a 25% solution of piperidine in DMF. Cleavage of the ivDde protecting group was performed using a solution of 5% hydrazine monohydrate in DMF. Finally, Boc-Glu(OBz)-OH (3 equiv) was coupled to the peptide-resin as described above. The resin was removed by filtration, and the amount of ivDde released into the filtrate was detected spectrophoto-

dx.doi.org/10.1021/bm500649q | *Biomacromolecules* XXXX, XXX, XXX−XXX

Table 2. Characteristics of *P*(HPMA) Conjugates

P(HPMA) conjugate	M_w	$Đ$	inhibitor content [wt %]	Dox content [wt %]
P-Ahx-NH-N═Dox	27 000	1.8		9.8
P-Ahx-NH-N═OPe-R121	33 100	1.12	10.8	
P-Ahx-NH-N═OHe-R121	33 100	1.12	12.5	
P-Ahx-NH-N═MeOHe-R121	33 100	1.12	8.6	
P-Ahx-NH-N═OPB-R121	29 600	1.13	7.8	
P-Ahx-NH-N═MeOHe-R121(Dox)	33 100	1.12	8.5	8.0
P-Ahx-R121	27 700	1.15	5.3	
P-Ahx-NH-NH-MeOHe-R121	33 100	1.12	9.2	
P-Ahx-NH-N═MeOHe-R205	30 700	1.06	7.0	
P-Ahx-NH-N═OPe-RIT	30 700	1.06	12.6	
P-Ahx-NH-N═OHe-RIT	30 700	1.06	18.3	
P-Ahx-NH-N═MeOHe-RIT	30 700	1.06	8.3	
P-Ahx-NH-N═OPB-RIT	30 700	1.06	18.8	
P-Ahx-NH-N═MeOHe-RIT(Dox)	31 900	1.09	7.3	9.4
P-Ahx-NH-NH-MeOHe-RIT	31 900	1.09	7.3	

metrically at 300 nm. Cleavage of the protected peptide methyl ester from the resin was performed using $Cu(OAc)_2$, pyridine and methanol as the nucleophile.[37] The product was triturated with diethyl ether and dried. The crude peptide derivative was purified chromatographically and characterized by HPLC and mass spectrometry.

The physicochemical characteristics of the derivatives of the ABC transporter inhibitors reversin 121, reversin 205 and ritonavir esters are summarized in Table 1.

Synthesis of *P*(HPMA) Precursor. The *P*(HPMA) precursors *P*-Ahx-NH-NH-Boc (here and in the following text, *P* indicates the HPMA copolymer backbone) with well-defined molecular weight and low polydispersity $Đ$ were prepared by reversible addition−fragmentation chain transfer (RAFT) polymerization by using chain transfer agent CTA and initiator AIBN. The ratio of monomer (M)/CTA was 400:1, and the ratio of CTA/AIBN was 3:1. An example of the polymerization follows: HPMA (1.0 g, 6.98 mmol), Ma-Ahx-NH-NH-Boc (0.243 g, 0.78 mmol), CTA (12.9 mg, 5.82×10^{-2} mmol), and AIBN (3.2 mg, 1.94×10^{-2} mmol) were dissolved in *t*-BuOH (2.33 mL). The solution was inserted into an ampule and bubbled with argon for 10 min. The ampule was sealed, and the polymerization was performed at 70 °C for 16 h. The polymer was isolated by precipitation into the mixture acetone/diethyl ether (3:1), filtered off, and dried under vacuum. The yield was 0.85 g (68.0%). The terminal dithio-benzoate group (DTB) was removed by the method described by Perrier et al.[38] The *P*(HPMA) precursor *P*-Ahx-NH-NH_2 was prepared by removing the Boc protecting group in the presence of TFA.[39]

Synthesis of *P*(HPMA) Conjugates with Inhibitor Derivatives. The *P*(HPMA) conjugates with inhibitor derivatives bound through pH-sensitive hydrazone bonds were prepared from the polymer precursor *P*-Ahx-NH-NH_2 (with reactive hydrazide groups in its side chains) by reaction with OPe-R121, OHe-R121, MeOHe-R121, OPB-R121, MeOHe-R205, OPe-RIT, OHe-RIT, MeOHe-RIT, or OPB-RIT.

An example of the synthesis of the polymer conjugate *P*-Ahx-NH-N═MeOHe-R121 follows: *P*-Ahx-NH-NH_2 (200 mg) was dissolved in dry methanol (1.2 mL), and MeOHe-R121 (25 mg) was added, followed by the addition of acetic acid (10 μL). The reaction mixture was stirred for 16 h at room temperature. The reaction mixture was then diluted with dry methanol (2 mL), and the conjugate P-Ahx-NH-N═MeOHe-R121 was purified by column chromatography on a Sephadex LH-20 column in methanol with UV detection at 220 nm. The compound was precipitated into ethyl acetate, isolated by filtration, and dried under vacuum.

The polymer conjugate *P*-Ahx-NH-NH-MeOHe-R121 was prepared by the reaction of *P*-Ahx-NH-N═MeOHe-R121 with cyanoborohydride. The conjugate *P*-Ahx-NH-N═MeOHe-R121 (50 mg) was dissolved in PBS buffer. Cyanoborohydride (20 mg) was added, and the pH was adjusted to 6.0. The reaction mixture was stirred for 6 h at room temperature. The conjugate *P*-Ahx-NH-NH-MeOHe-R121 was purified on a PD-10 column with water as the mobile phase and lyophilized. The yield was 47 mg.

The polymer conjugate *P*-Ahx-R121 was prepared by copolymerization of HPMA (0.2 g) and Ma-Ahx-R121 (0.112 g) by RAFT polymerization using the chain transfer agent CTA and the initiator AIBN.

The conjugate *P*-Ahx-NH-N═Dox was prepared by the reaction of the precursor *P*-Ahx-NH-NH_2 with Dox·HCl in methanol in the dark and was purified as described earlier.[40] The characteristics of the *P*(HPMA) conjugates are summarized in Table 2.

Synthesis of *P*(HPMA) Conjugates with Inhibitor Derivatives and Doxorubicin. The conjugate *P*-Ahx-NH-N═MeOHe-R121(Dox) was prepared by reaction of the precursor *P*-Ahx-NH-NH_2 (50 mg) with MeOHe-R121 (10 mg) in dry methanol in the presence of acetic acid (4 μL). The reaction was carried out for 16 h. Dox·HCl (5 mg) was then added, and the reaction mixture was stirred for 24 h. The reaction mixture was diluted with dry methanol (2 mL), and the conjugate *P*-Ahx-NH-N═MeOHe-R121(Dox) was purified by column chromatography on a Sephadex LH-20 column with methanol as the mobile phase. It was then precipitated into ethyl acetate, isolated by filtration, and dried under vacuum. The yield was 48 mg of *P*-Ahx-NH-N═MeOHe-R121(Dox).

Characterization of Monomers, *P*(HPMA) Precursor, and *P*(HPMA) Conjugates. The monomers and inhibitor derivatives were characterized using a HPLC Shimadzu system with a reverse-phase column (Chromolith HighResulution RP-18e, 100 × 4.6 mm) (Merck, Germany) equipped with a UV/vis photodiode array detector. Gradient elution with 5−95% of acetonitrile for 15 min at a flow rate of 1.0 mL/min was used. The molecular weights of the monomers and inhibitors were determined using a mass spectrometer (MS LCQ Fleet, Thermo Fisher Scientific). The structures were confirmed by ^{1}H NMR (300 MHz) using a Bruker DPX 300 spectrometer and by elemental analysis.

The number-average molecular weights (M_n), weight-average molecular weights (M_w), and polydispersities ($Đ$) of the polymer precursors and *P*(HPMA) conjugates were measured using size-exclusion chromatography (SEC) on a HPLC Shimadzu system equipped with a UV detector, an Optilab rEX differential refractometer, and multiangle light scattering DAWN 8 (Wyatt Technology) detector. For these experiments, a 20% 0.3 M acetate/80% methanol (v/v) buffer and either a TSKgel G3000SW or a TSKgel G4000SW column were used.

The content of the inhibitor in the polymer conjugates was determined by amino acid analysis of the hydrolyzed *P*(HPMA) conjugates (6 M HCl, 115 °C, 18 h in a sealed ampule) using a reverse-phase column (Chromolith HighResulution RP-18e, 100 × 4.6 mm) (Merck, Germany) after precolumn derivatization with phthalaldehyde (OPA) and 3-sulfanylpropanoic acid (excitation at

dx.doi.org/10.1021/bm500649q | *Biomacromolecules* XXXX, XXX, XXX−XXX

229 nm, emission at 450 nm). Gradient elution with 10−100% solvent B for 35 min at a flow rate of 1.0 mL/min was used, where solvent A was 0.05 M sodium acetate buffer, pH 6.5, and solvent B was 300 mL of 0.17 M sodium acetate and 700 mL of methanol.

The Dox content was determined spectrophotometrically on a Specord 205 (Jena Analytics) spectrophotometer (ε_{488} = 10 700 L·mol^{-1}·cm^{-1}; methanol), and the content of the hydrazide groups was determined by the TNBSA method (ε_{500} = 17 550 L·mol^{-1}·cm^{-1}; borate buffer pH 9.3).[40]

In Vitro Release of the ABC Transporter Inhibitors and Dox from the *P*(HPMA) Conjugates. The rate of release of the derivatives of reversin 121, reversin 205, and ritonavir esters from the *P*(HPMA) conjugates was investigated by incubation of the conjugates in phosphate buffers at pH 5.0 or 7.4 (0.1 M phosphate buffer with 0.05 M NaCl) at 37 °C. An example of a release experiment follows: the conjugate *P*-Ahx-NH-N═MeOHe-R121 (10.5 mg, 1.3 mM MeOHe-R121) was dissolved in phosphate buffers at either pH 5.0 or pH 7.4. The stock solutions (0.3 mL) were placed in Eppendorf vials and incubated at 37 °C. At predetermined time intervals, chloroform (0.4 mL) was added to the vial and the mixture was vortexed for 2 min. The chloroform layer (0.3 mL) was transferred into a new vial. The residue, after evaporation of the chloroform, was dissolved in methanol (0.1 mL), and the amount of released MeOHe-R121 was determined by HPLC analysis performed on an HPLC instrument (Shimadzu, Japan) using a reverse-phase column (Chromolith Performance RP-18e; 100 × 4.6 mm) with UV detection at 220 and 260 nm. The mobile phase was water−methanol with a methanol gradient of 20−100 vol %, and the flow rate was 1.0 mL/min. All release data are expressed as the percentage of the amount of the free inhibitor derivative (drug) relative to the total inhibitor derivative (drug) content in the polymer conjugate. All experiments were carried out in triplicate.

Cell Lines and Cell Cultures. The murine monocytic leukemia cell line P388 (parental cell line) and its doxorubicin-resistant subline P388/MDR (a cell line that overexpresses P-gp) were obtained from Prof. I. Lefkovits (Basel Institute for Immunology, Basel, Switzerland). Both cell lines were propagated in RPMI-1640 medium supplemented with heat-inactivated 10% fetal calf serum (FCS), 2 mM glutamine, 100 U/mL penicillin, 1 mM sodium pyruvate, 100 μg/mL streptomycin, and 5 mL nonessential amino acids (Sigma-Aldrich, Czech Republic). The P388/MDR cells were grown in the continuous presence of 750 ng/mL doxorubicin to maintain the MDR-phenotype. One day before each experiment, the cells were transferred to doxorubicin-free culture medium. Both cell lines were propagated at 37 °C in a 5% CO_2 atmosphere. The cell lines were tested for mycoplasma infection (MycoAlert Mycoplasma Detection kit, Lonza, Switzerland).

Cellular Drug Sensitivity Assay. To test the cytostatic effect of the drugs in the presence or absence of chemosensitizers, cell growth inhibition was determined using the [^{3}H]-thymidine incorporation assay. The cells (1 × 10^4 per well) were seeded into 96-well flat bottom (FB) tissue culture plates (Nunc, Denmark). Various concentrations of the samples were added to the wells to reach a final volume of 250 μL. Triplicate wells were used for each test condition. The plates were incubated in 5% CO_2 at 37 °C for 72 h. After this incubation, each well was pulsed with 1 μCi (37 kBq) of [^{3}H]-thymidine for 6 h. The cells were then collected on glass fiber filters (Filtermat, Wallac, Finland) using a cell harvester (Tomtec), and the radioactivity of the samples was measured in a scintillation counter (1450 MicroBeta TriLux, Wallac, Finland). Cells cultivated in fresh medium were used as controls. The inhibition of tumor cell growth is expressed as the IC_{50}, that is, the concentration of Dox (or equivalent) that inhibited cell growth by 50%. All reported IC_{50} values are the mean of at least three independent experiments. The resistance ratio was calculated by dividing the IC_{50} value for the P388/MDR cell line by the corresponding value in the P388 cells.

Calcein Efflux Assay. The calcein assay was performed using 96-well round-bottom (U-base) tissue culture plates (TPP, Switzerland). All incubation steps were conducted in 5% CO_2 at 37 °C. The drug-sensitive and drug-resistant cells were seeded at a concentration of 1 × 10^5 cells per well (100 μL per well) in culture medium. The cells were then incubated with the tested compounds or controls (in duplicates) for 30 min. After this preincubation, calcein acetoxymethyl ester (calcein-AM) was added (final concentration 0.1 μM), and the cells were incubated for another 20 min in the dark. After this 20 min incubation, the uptake of calcein-AM was terminated by centrifugation (200*g*, 5 min, at 4 °C). The cell pellets were washed and centrifuged twice with 200 μL and then resuspended in 100 μL of cold FACS buffer (PBS with 2% FCS and 2 mmol EDTA). The flow cytometric analysis was performed using an LSRII instrument (BD Biosciences), and the data were analyzed using FlowJo software (Tree Star, Inc.). Nonliving cells were detected and gated out using Hoechst 33258 staining (Sigma-Aldrich, Czech Republic). Each experiment was performed at least three times.

Statistical Analysis. The data from the various experiments are reported as the means ± standard deviation (SD). For statistical analysis, Student's *t* test for independent measurements was used. A value of $P < 0.05$ was considered significant.

RESULTS AND DISCUSSION

Two cell lines, normal murine leukemia cell line P388 and its Dox-resistant subline P388/MDR (for detailed characteristics, see Materials and Methods), were used to study the biological effects of the selected P-gp inhibitors, their derivatives, and their *P*(HPMA) conjugates. P388 cells are sensitive to Dox, a cytostatic drug used in our study, which shows an IC_{50} of approximately 0.01 μM (Supporting Information Table 1). The P388/MDR cell line is highly resistant to Dox, with an IC_{50} of approximately 5.9 μM. Thus, the P388/MDR cells are approximately 600 times less sensitive to Dox than the parental P388 cell line. A similar situation is observed when the *P*-Ahx-NH-N═Dox conjugate is used instead of free Dox: the IC_{50} concentrations for the P388 and P388/MDR cells are 0.024 and 92 μM, respectively. The calculated resistance ratio for *P*-Ahx-NH-N═Dox is thus approximately 3800, even higher than that for free Dox. The higher resistance ratio found for P-Ahx-NH-N═Dox than for free Dox may be explained by lower intracellular concentration of Dox released from *P*-Ahx-NH-N═Dox entering the cell by slower endocytosis in comparison with fast diffusion of free Dox which results in its more effective efflux by P-gp and in this consequence also lower cytotoxicity of the conjugate.

Synthesis of *P*(HPMA) Conjugates with Inhibitor Derivatives and Doxorubicin. To increase the cytostatic activity of free Dox and polymer conjugate P-Ahx-NH-N═Dox in the Dox-resistant P388/MDR cell line, we synthesized novel polymeric therapeutics based on HPMA copolymers bearing either the anticancer drug, an inhibitor of ABC transporters or both. The ABC transporter inhibitors selected for this study were reversin 121, reversin 205 and ritonavir. Reversin 121 (Boc-Asp(OBzl)-Lys(Z)-OtBu) and reversin 205 (N^{α},N^{ε}-bis-[Boc-Glu(OBzl)-Lys-OMe) exhibit good affinity and specificity for P-gp,[9,10,41] but these compounds do not contain any groups suitable for covalent attachment to the HPMA copolymer. The synthesis of derivatives of reversin 121 in which the Boc protecting group was substituted with 4-oxopentanoate, 6-oxoheptanoate, 5-methyl-4-oxohexanoate, and 4-(2-oxopropyl)-benzoate enabled conjugation of these derivatives to the *P*(HPMA) precursor bearing hydrazide groups via a pH-sensitive hydrazone bond. This process is shown in Scheme 1. The derivatives of ritonavir were prepared by esterification of the ritonavir hydroxyl group with 4-oxopentanoic acid, 6-oxoheptanoic acid, 5-methyl-4-oxohexanoic acid, and 4-(2-oxopropyl)-benzoic acid as shown in Scheme 2. Reversin 205

dx.doi.org/10.1021/bm500649q | *Biomacromolecules* XXXX, XXX, XXX−XXX

derivatized with 5-methyl-4-oxohexanoic acid was prepared using manual solid phase peptide synthesis, as shown in Scheme 3. Substituents differing in their detailed structure were selected to facilitate control of the rate of hydrolysis of the hydrazone bond (the bond used for their attachment to the polymer) and thus the rate of release of the derivatives of inhibitors from the polymer carrier. The detailed procedures for the synthesis of all inhibitor derivatives are described above and the physicochemical characteristics of the derivatives of the inhibitors are summarized in Table 1.

The *P*(HPMA) precursor containing hydrazide groups was prepared by RAFT copolymerization of HPMA and Ma-Ahx-NH-NH-Boc. The RAFT copolymerization enabled the synthesis of polymer precursors with well-defined molecular weights and low polydispersities (*Đ*). The terminal dithiobenzoate group (DTB) was removed using the method described by Perrier et al.[38] The precursor *P*-Ahx-NH-NH_2 was prepared by removing the Boc protecting group from the copolymer hydrazide groups in the presence of TFA.[39]

P(HPMA) conjugates containing derivatives of the inhibitors were prepared by the reaction of the hydrazide groups of the precursor *P*-Ahx-NH-NH_2 with the carbonyl group of the oxoacid-derivatized inhibitors or with Dox in methanol in the presence of a trace of acetic acid. The content of the inhibitors and Dox in the conjugates was controlled by the amount of inhibitor derivative or Dox added to the reaction mixture and by the amount of hydrazide groups in the precursor. In addition to the conjugates described above, *P*(HPMA) conjugates containing the inhibitors bound to the copolymer precursor via nondegradable bonds were also prepared. The first type of conjugates, *P*-Ahx-R121 and *P*-Ahx-RIT, was prepared by copolymerization of HPMA with monomers Ma-Ahx-R121 or Ma-Ahx-RIT, respectively, and the second type of conjugates, *P*-Ahx-NH-NH-R121 and *P*-Ahx-NH-NH-RIT, was prepared by reduction of the hydrazone bond with cyanoborohydride. The characteristics of the *P*(HPMA) conjugates with all of the inhibitors are summarized in Table 2.

In Vitro Release of Inhibitor Derivatives from *P*(HPMA) Conjugates. The in vitro release profiles of the derivatives of reversin 121 and reversin 205 from *P*(HPMA) conjugates at pH 5.0 and 7.4 (37 °C) are shown in Figure 1. The rates of release at pH 7.4 are much lower than those at pH 5.0. These results agree well with our earlier measurements of the release rates of various drugs (dexamethasone, derivatives of paclitaxel, docetaxel, or mitomycin C) from *P*(HPMA) conjugates bearing the drugs bound via hydrazone bonds.[42−44] After 24 h of incubation of the *P*-Ahx-NH-N═MeOHe-R121 conjugate at pH 5.0, 90% of the MeOHe-R121 was released, while at pH 7.4 only 3% of the MeOHe-R121 was released after the same incubation time.

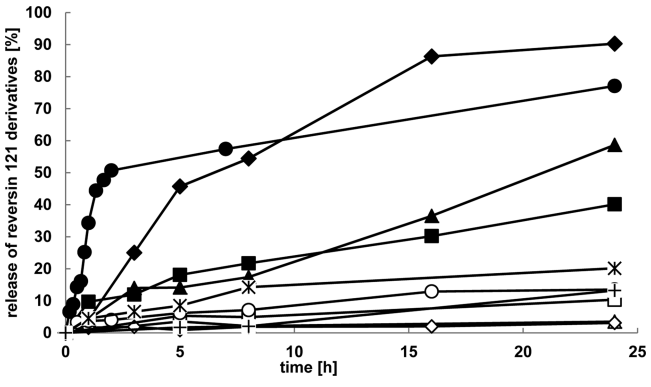

Figure 1. Release of derivatives of reversin 121 and reversin 205 from polymer conjugates. At pH 5.0: (◆) MeOHe-R121; (■) OHe-R121; (▲) OPe-R121; (∗) OPB-R121; (●) MeOHe-R205. At pH 7.4: (◇) MeOHe-R121; (□) OHe-R121; (△) OPe-R121; (+) OPB-R121; (○) MeOHe-R205.

The in vitro release experiments performed with the conjugates *P*-Ahx-NH-N═MeOHe-R121, *P*-Ahx-NH-N═OHe-R121, *P*-Ahx-NH-N═OPe-R121, and *P*-Ahx-NH-N═OPB-R121 showed that the rate of release of MeOHe-R121, OHe-R121, OPe-R121, and OPB-R121 is controlled by the structure of the oxoacids used for the derivatization of reversin 121. After 24 h of incubation at pH 5.0, the amounts of the reversin 121 derivatives released from the *P*(HPMA) conjugates decrease in the order of MeOHe-R121 (90%), OPe-R121 (59%), OHe-R121 (40%), and OPB-R121 (20%).

Additionally, the release profiles obtained for the polymer conjugates *P*-Ahx-NH-N═OHe-R121, *P*-Ahx-NH-N═OPe-R121, and *P*-Ahx-NH-N═OPB-R121 showed that the rates of release of the inhibitor derivatives at pH 7.4 are much lower than those at pH 5.0. After 24 h of incubation at pH 7.4, only 3% of OPe-R121, 10% of OHe-R121, and 13% of OPB-R121 were released.

No release of R121 and MeOHe-R121 from the polymer conjugates *P*-Ahx-R121, *P*-Ahx-NH-NH-MeOHe-R121 was observed in buffer at pH 5.0 at 37 °C.

The in vitro release experiment carried out with the polymer conjugate *P*-Ahx-NH-N═MeOHe-R205 showed that, after 2 h incubation at pH 5.0, 50% of the MeOHe-R205 was released. After 24 h incubation at pH 5.0, 77% of the MeOHe-R205 was released from the polymer conjugate, while at pH 7.4 only 13% of the MeOHe-R205 was released.

The in vitro release profiles of the RIT esters from the *P*(HPMA) conjugates at pH 5.0 and 7.4 (37 °C) are shown in Figure 2. The release profiles obtained for the conjugates *P*-Ahx-NH-N═OPe-RIT, *P*-Ahx-NH-N═MeOHe-RIT, *P*-Ahx-NH-N═OHe-RIT, and *P*-Ahx-NH-N═OPB-RIT show that the rates of release of the RIT esters at pH 7.4 are much lower than those at pH 5.0. The rates of release of the RIT esters are controlled by the structure of the oxoacids used for the esterification of the RIT. After 24 h incubation at pH 5.0, the amounts of RIT esters released decrease in the order of

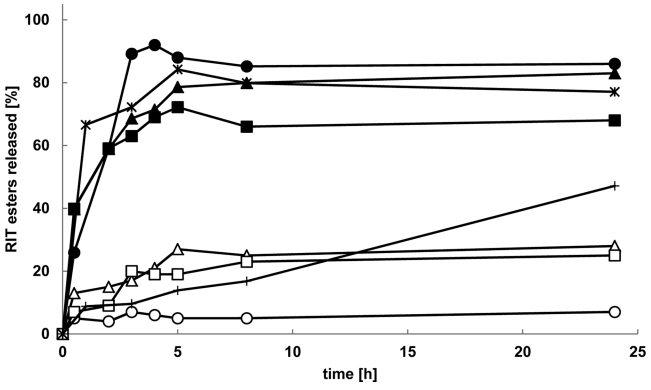

Figure 2. Release of ritonavir esters from *P*(HPMA) conjugates. At pH 5.0: (●) MeOHe-RIT; (▲) OPe-RIT; (∗) OHe-RIT; (■) OPB-RIT. At pH 7.4: (○) MeOHe-RIT; (△) OPe-RIT; (+) OHe-RIT; (□) OPB-RIT.

dx.doi.org/10.1021/bm500649q | *Biomacromolecules* XXXX, XXX, XXX−XXX

MeOHe-RIT (86%), OPe-RIT (83%), OHe-R121 (77%), and OPB-R121 (68%).

The release profile obtained for the conjugate *P*-Ahx-NH-N═MeOHe-RIT shows that the rate of MeOHe-RIT release at pH 7.4 is much lower than that at pH 5.0. After 24 h of iincubation at pH 7.4, only 7% of MeOHe-RIT were released. The rates of release of OPe-RIT, OHe-RIT, and OPB-RIT from the conjugates *P*-Ahx-NH-N═OPe-RIT, *P*-Ahx-NH-N═OHe-RIT, and *P*-Ahx-NH-N═OPB-RIT were higher than those for the release of MeOHe-RIT from the conjugate *P*-Ahx-NH-N═MeOHe-RIT at pH 7.4. After 24 h of incubation at pH 7.4, 28% of OPe-RIT, 47% of OHe-RIT, and 25% of OPB-R121 were released from their respective conjugates.

Hydrolysis of the ester bond and release of RIT from the RIT esters were not detected after 24 h incubation at pH 7.4. No release of RIT or MeOHe-RIT from the polymer conjugates *P*-Ahx-RIT and *P*-Ahx-NH-NH-MeOHe-RIT was observed after 24 h in a buffer at pH 5.0 at 37 °C.

Prerequisites for effective intracellular delivery of derivatives of MDR inhibitors are stability of their polymer conjugates during transport in the blood circulation, as simulated here by incubation in a phosphate buffer at pH 7.4, and rapid release at the site of action as simulated by incubation in a phosphate buffer at pH 5.0. The conjugates *P*-Ahx-NH-N═MeOHe-R121 and *P*-Ahx-NH-N═MeOHe-RIT fulfill these requirements best, because they show the largest difference between their good stability in buffer solution at pH 7.4 and rapid inhibitor release at pH 5.0. For this reason, these *P*(HPMA) conjugates were selected for further in vitro biological evaluation.

In Vitro Toxicity and Inhibitory Activity of Selected P-gp Inhibitors and Their Derivatives. First, the in vitro toxicities and activities of the original inhibitors, reversin 121, reversin 205, and ritonavir, were evaluated and compared with the activities of the derivatives of these agents suitable for conjugation to the *P*(HPMA) carrier. The derivatives of the P-gp inhibitors were intended to induce sensitization of the MDR cancer cells to the cytostatic effect of Dox. However, it was important that the concentration used did not affect the proliferation of MDR cells per se. Thus, both P388 and P388/MDR cells were incubated with titrated concentrations of the tested compounds, and the IC_{50}'s were determined by the standard [^{3}H]-thymidine incorporation assay. The results are summarized in Table 3.

All reversin 121 derivatives except for OPe-R121, which showed no toxicity in either cell line within the concentration range used, exerted toxicity comparable to unmodified reversin 121 in the P388 cell line. However, MeOHe-R121, OHe-R121, and OPB-R121 showed approximately 2.5−4 times lower toxicity than reversin 121 in the P388/MDR cell line. Notably, reversin 121 was more than 2-fold more toxic to the P388/MDR cells than the P388 cells. Conversely, reversin 205 was almost 6 times less toxic to the P388/MDR cells than to the P388 cells. MeOHe-R205 was less toxic than parent compound in both cell lines; however, the decrease in toxicity was much more pronounced in the P388 cells (∼6 times versus 1.5 times). Ritonavir, the last P-gp inhibitor tested, was approximately 3.5 times less toxic to the P388/MDR cells than to the P388 cells. All ritonavir esters were shown to have comparable or only slightly lower (up to 1.5 times) toxicity in the P388 cell line. On the other hand, OHe-RIT and MeOHe-RIT showed 2-fold higher toxicity and OPB-RIT showed 2-fold lower toxicity than the parent compound in the P388/MDR cell line.

Table 3. IC_{50}'s of Different Inhibitors of P-gp Determined after Culture with the Sensitive (P388) and Multidrug-Resistant (P388/MDR) Cell Lines

P-gp inhibitor and derivatives	P388 IC_{50} (μM)[a]	P388/MDR IC_{50} (μM)
reversin 121	12.1 ± 1.45	5.5 ± 0.74
OPe-R121	>32	>32
OHe-R121	11.9 ± 1.65	21.5 ± 1.00
MeOHe-R121	10.6 ± 1.75	15.3 ± 2.66
OBP-R121	23.0 ± 0.50	14.1 ± 2.03
reversin 205	3.9 ± 0.25	22.7 ± 0.20
MeOHe-R205	13.2 ± 0.60	34.3 ± 0.80
ritonavir	7.2 ± 0.72	24.9 ± 1.02
OHe-RIT	11.1 ± 0.76	14.2 ± 0.56
MeOHe-RIT	9.1 ± 0.82	12.4 ± 1.40
OPB-RIT	11.5 ± 1.50	43.0 ± 1.00

[a] IC_{50} (μM) values were calculated as the concentration of the tested P-gp inhibitor or its derivative which inhibited the incorporation of [^{3}H]-thymidine into the exposed cells to 50% of the controls after 72 h of culture (see Materials and Methods). The activity of control cells was always greater than 50 000 cpm/well. The experiments were repeated 2−6 times, and the average values ± SE are shown.

The compounds described above were then tested for their potential to inhibit the drug-efflux function of P-gp using the calcein assay. Of the derivatives of reversin 121 tested, MeOHe-R121 showed exceptionally high inhibitory activity (Figure 3A). In fact, MeOHe-R121 was found to be even more potent as a P-gp inhibitor than the unmodified reversin 121. Thus, MeOHe-R121 was the first promising candidate compound as a potent P-gp inhibitor, and it is possible to conjugate it to the HPMA copolymer via hydrazone bonds. Moreover, MeOHe-R121 is approximately 3 times less toxic than reversin 121 in the P388/MDR cells, and it shows very good P-gp inhibitory activity at a concentration of 4 μM, which is far below its IC_{50} in these cells. In contrast to the reversin 121 derivatives, MeOHe-R205 showed no P-gp inhibitory activity at all (Figure 3B). MeOHe-RIT was identified to be a potent inhibitor of P-gp function, while the other tested ritonavir esters were significantly less potent (Figure 3C). As it was observed for MeOHe-R121, MeOHe-RIT was also found to be even more potent as a P-gp inhibitor than the unmodified ritonavir. However, the toxicity of MeOHe-RIT is slightly higher and the P-gp inhibitory activity is somewhat lower than that found for MeOHe-R121. Thus, MeOHe-RIT was selected as another candidate for further studies even though its expected activity is slightly lower than that of MeOHe-R121. Interestingly, of the nine derivatives of three different P-gp inhibitors, the two most promising candidates were both obtained through modification with 5-methyl-4-oxoheptanoic acid.

Sensitization of P388/MDR Cells to the Cytostatic Activity of Dox by Selected P-gp Inhibitors and Their Derivatives in Vitro. To evaluate the potential for the selected P-gp inhibitors and their derivatives to overcome multidrug resistance in the P-gp-overexpressing P388/MDR cells as measured by the cytostatic effect of Dox, the cells were incubated with titrated concentrations of the P-gp inhibitors or their derivatives at a constant concentration of Dox (2 μM). This concentration of Dox (∼3 times lower than IC_{50}) has only negligible cytostatic activity in the P388/MDR cells. MeOHe-R121 showed the highest capacity to sensitize P388/MDR cells to Dox among all of the derivatives of reversin 121 tested (Figure 4A). The activity of MeOHe-R121 was comparable to

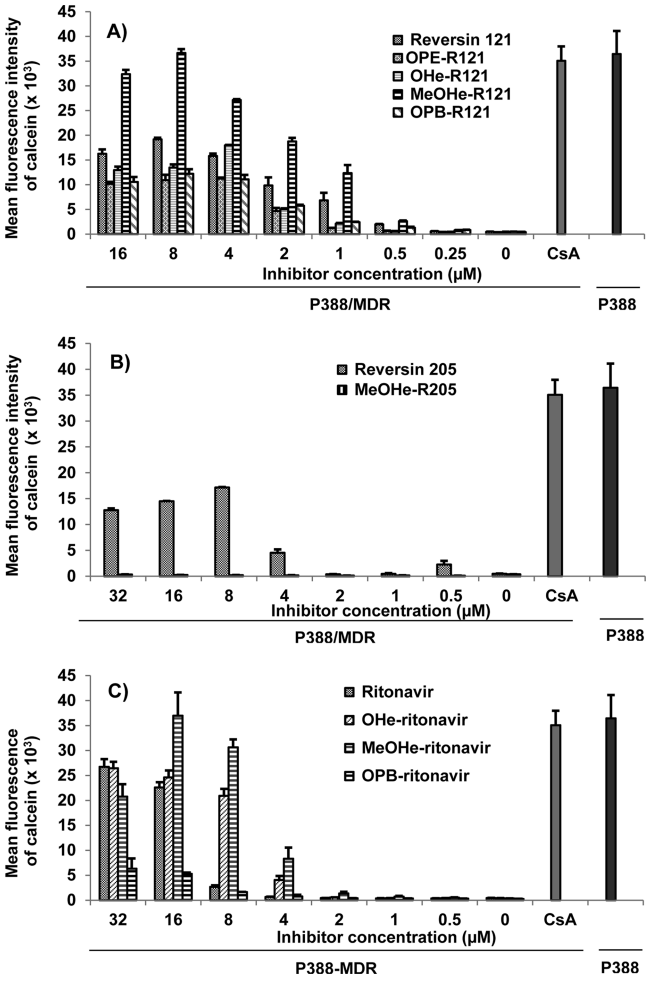

Figure 3. Inhibition of P-gp function by reversin 121 (A), reversin 205 (B), and ritonavir (C) and their derivatives in P388/MDR cells. The P388/MDR cells were incubated with titrated concentrations of the P-gp inhibitors or their derivatives for 30 min under standard culture conditions. Calcein-AM was then added and the cells were incubated for another 20 min. The cells were analyzed by flow cytometry for calcein fluorescence, and the dead cells were gated out using Hoechst 33258. P388/MDR cells incubated with 10 μM cyclosporine A (CsA) and P388 cells incubated with calcein-AM only were used as positive controls. The values shown are the averages of three to six experiments ± SD.

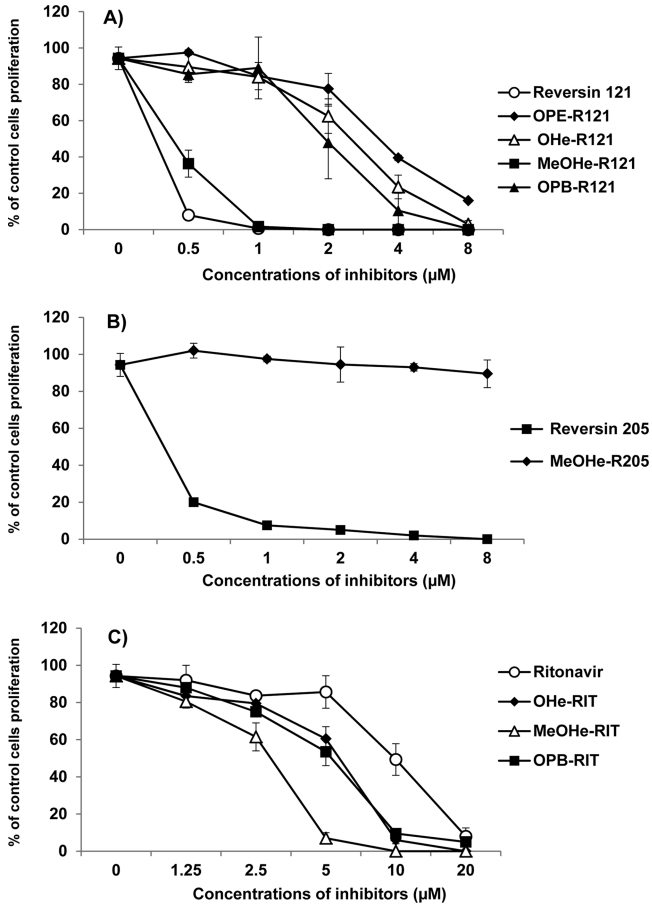

Figure 4. Sensitization of P388/MDR cells to the cytostatic effect of Dox by reversin 121 (A), reversin 205 (B), ritonavir (C), and their derivatives. P388/MDR cells were incubated with titrated concentrations of P-gp inhibitors or their derivatives and a constant concentration of Dox (2 μM) for 72 h under standard culture conditions. The cell proliferation was assessed by [^{3}H]-thymidine incorporation by adding this tracer to the cultures for last 6 h of incubation. The results are shown as the inhibition of the proliferation of the exposed cells relative to the controls (cells incubated in medium only). The activity of the control cells was always greater than 50 000 cpm/well. Each experimental point is the average of three experiments ± SD.

the unmodified reversin 121 and it was evident at concentrations of as low as 0.5 μM. Proliferation was completely inhibited when the P388/MDR cells were exposed to 1 μM MeOHe-R121. OPe-R121, OHe-R121, and OPB-R121 were much less potent, as demonstrated by the complete or near complete inhibition of proliferation at concentrations as high as 8 μM. Reversin 205 showed potency similar to that of reversin 121 in sensitizing the P388/MDR cells to Dox. However, its derivative, MeOHe-R205, was totally inactive (Figure 4B). Ritonavir and its esters were generally much less efficient in sensitizing the P388/MDR cells to Dox in comparison to reversin 121 (Figure 4C). Nevertheless, MeOHe-RIT showed reasonable activity, as demonstrated by the observation that it caused nearly complete inhibition of the proliferation at 5 μM. Of note, MeOHe-RIT was shown to be significantly more potent (~4 times) than the parent compound ritonavir. The IC_{50}'s for Dox in the presence of titrated concentrations of reversin 121, reversin 205, ritonavir, and their derivatives are summarized in Supporting Information Tables 2–4. In conclusion, this study on the sensitization of the P388/MDR cells to Dox treatment is in good agreement with the results of the calcein assay experiments and identifies two compounds, MeOHe-R121 and MeOHe-RIT, as promising candidates for the subsequent study aimed at conjugation of these inhibitors to the *P*(HPMA) carrier.

The effects of 1,7-substituted 3-*n*-propylxanthine derivatives at 100 μM concentration on the influx and efflux of Dox in P388 and P388/MDR leukemia cells were studied by Sadzuka et al.[45] The substituents in position 7, 3′-dimethylaminopropyl and 3′-hydroxypropyl, significantly inhibited the Dox efflux from P388 cells. In P388/MDR cells, most substituents in positions 1 and 7 had no effect on Dox efflux except for the 3′-dimethylaminopropyl derivative which facilitated influx of Dox and inhibited its efflux in a dose-dependent manner. Unfortunately, no experiments dealing with polymer conjugates of these inhibitors were described.

dx.doi.org/10.1021/bm500649q | *Biomacromolecules* XXXX, XXX, XXX–XXX

In Vitro Toxicity and P-gp Inhibitory Activity of the *P*(HPMA) Conjugates *P*-Ahx-NH-N═MeOHe-R121 and *P*-Ahx-NH-N═MeOHe-RIT. The polymer conjugates *P*-Ahx-NH-N═MeOHe-R121 and *P*-Ahx-NH-N═MeOHe-RIT, containing MeOHe-R121 or MeOHe-RIT, respectively, linked to the carrier via a pH-sensitive hydrazone bond, were synthesized. Their toxicity toward the P388/MDR cells was tested in a manner similar to the method used for the selected P-gp inhibitors and their derivatives. The *P*(HPMA) conjugate *P*-Ahx-NH-N═MeOHe-R121 showed no toxicity up to 24 μM (the concentrations stated hereafter are those of the active compound), and only modest toxicity was observed at 48 μM, the highest concentration tested (Figure 5A). The *P*-Ahx-NH-NH-MeOHe-R121and *P*-Ahx-R121 conjugates containing MeOHe-R121 or reversin 121, respectively, bound to the *P*(HPMA) carrier via a nonbiodegradable bond were used as controls and showed no toxicity. In contrast, the *P*-Ahx-NH-N═MeOHe-RIT polymer conjugate was significantly toxic at 48 and 24 μM. However, at concentrations up to 12 μM, this conjugate showed no or negligible toxicity (Figure 5B). *P*-Ahx-NH-NH-MeOHe-RIT and *P*-Ahx-RIT conjugates containing MeOHe-RIT or RIT, respectively, bound to the *P*(HPMA) carrier via nonbiodegradable bonds were used as controls and showed no toxicity. Furthermore, the *P*-Ahx-NH-N═MeOHe-R121 and *P*-Ahx-NH-N═MeOHe-RIT conjugates were tested for their potential to inhibit the drug-efflux function of P-gp using the calcein assay. The P388/MDR cells were preincubated with the tested conjugates for 16 h, after which the cells were used in the standard calcein assay. Both conjugates, *P*-Ahx-NH-N═MeOHe-R121 and *P*-Ahx-NH-N═MeOHe-RIT, showed very good P-gp inhibitory activity at 12 μM, but lower concentrations were only partially effective (Figure 6). None of the control *P*(HPMA) conjugates described above (Figure 5) showed any activity.

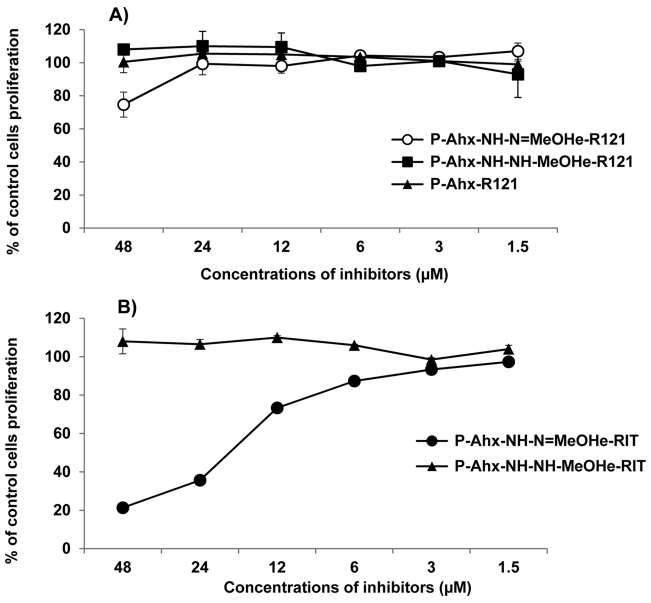

Figure 5. Toxicity of *P*(HPMA) conjugates *P*-Ahx-NH-N═MeOHe-R121, *P*-Ahx-NH-NH-MeOHe-R121, and *P*-Ahx-R121 (A), and *P*-Ahx-NH-N═MeOHe-RIT and *P*-Ahx-NH-NH-MeOHe-RIT (B) as indicated by inhibition of the proliferation of the P388/MDR cells. The P388/MDR cells were incubated with titrated concentrations of the *P*(HPMA) conjugates *P*-Ahx-NH-N═MeOHe-R121, *P*-Ahx-NH-NH-MeOHe-R121, *P*-Ahx-R121, *P*-Ahx-NH-N═MeOHe-RIT, and *P*-Ahx-NH-NH-MeOHe-RIT for 72 h under standard culture conditions. Cell proliferation was assessed using [^{3}H]-thymidine incorporation by adding this tracer to the cultures for the last 6 h of incubation. The results shown are the inhibition of the proliferation of the exposed cells relative to the controls (cells incubated in medium only). The activity of control cells was always greater than 50 000 cpm/well. Each experimental point is the average of three experiments ± SD.

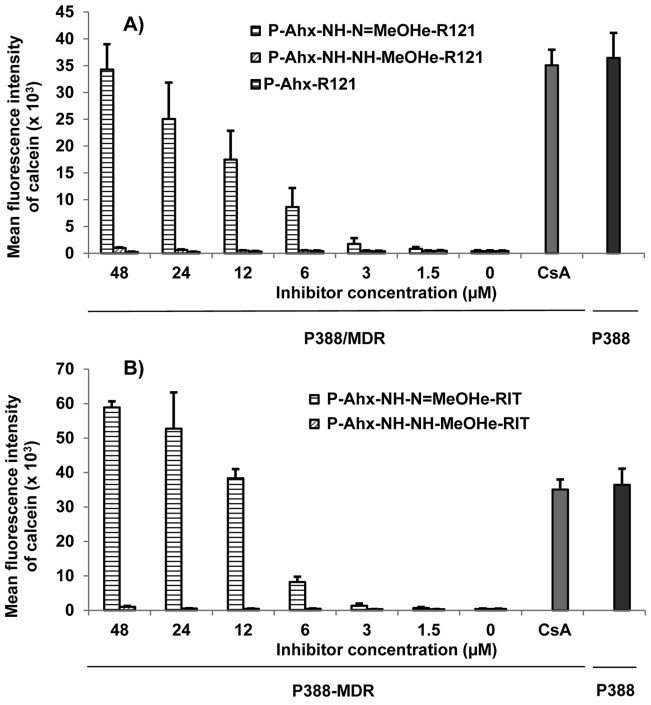

Figure 6. Ability of the *P*(HPMA) conjugates *P*-Ahx-NH-N═MeOHe-R121, *P*-Ahx-NH-NH-MeOHe-R121, and *P*-Ahx-R121 (A), and *P*-Ahx-NH-N═MeOHe-RIT and *P*-Ahx-NH-NH-MeOHe-RIT (B) to inhibit P-gp function in the P388/MDR cells. P388/MDR cells were incubated with titrated concentrations of the *P*(HPMA) conjugates *P*-Ahx-NH-N═MeOHe-R121, *P*-Ahx-NH-NH-MeOHe-R121, *P*-Ahx-R121, *P*-Ahx-NH-N═MeOHe-RIT, and *P*-Ahx-NH-NH-MeOHe-RIT for 16 h under standard culture conditions. Calcein-AM was then added, and cells were incubated for another 30 min. The cells were analyzed by flow cytometry for calcein fluorescence, and the dead cells were gated out using Hoechst 33258. P-388/MDR cells incubated with 10 μM cyclosporine A (CsA) and P388 cells incubated with calcein-AM only were used as positive controls. The values shown are the averages of three experiments ± SD.

Sensitization of P388/MDR Cells to the Cytostatic Activity of Dox by the *P*(HPMA) Conjugates *P*-Ahx-NH-N═MeOHe-R121 and P-Ahx-NH-N═MeOHe-RIT in vitro. To evaluate the potential for the polymer conjugates *P*-Ahx-NH-N═MeOHe-R121 and *P*-Ahx-NH-N═MeOHe-RIT to overcome multidrug resistance in the P-gp overexpressing P388/MDR cells, as indicated by the cytostatic effect of Dox, the cells were incubated with titrated concentrations of Dox and with various concentrations of these conjugates. The concentrations selected for conjugates *P*-Ahx-NH-N═MeOHe-R121 and *P*-Ahx-NH-N═MeOHe-RIT were 24 and 12 μM, respectively, because higher concentrations were found to be toxic.

The *P*-Ahx-NH-N═MeOHe-R121 conjugate showed a gradually increasing capacity to sensitize the P388/MDR cells

dx.doi.org/10.1021/bm500649q | *Biomacromolecules* XXXX, XXX, XXX−XXX

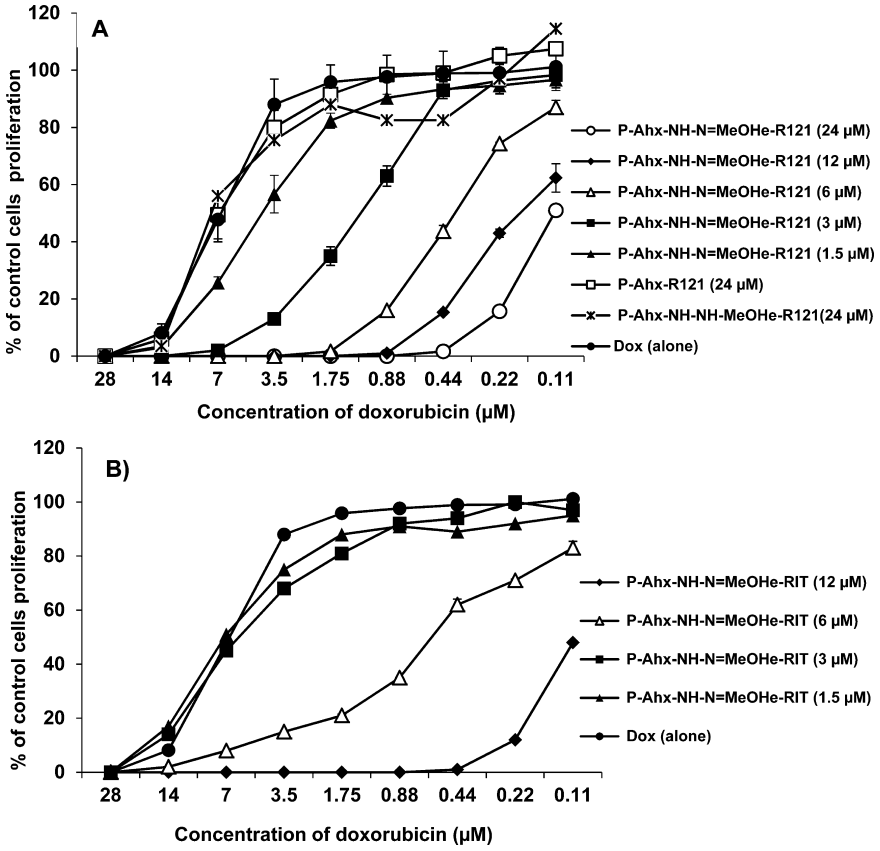

Figure 7. Sensitization of P388/MDR cells to the cytostatic effect of doxorubicin by the *P*(HPMA) conjugates *P*-Ahx-NH-N═MeOHe-R121, *P*-Ahx-NH-NH-MeOHe-R121, and *P*-Ahx-R121 (A), and *P*-Ahx-NH-N═MeOHe-RIT and *P*-Ahx-NH-NH-MeOHe-RIT (B). P388/MDR cells were incubated with titrated concentrations of the *P*(HPMA) conjugates *P*-Ahx-NH-N═MeOHe-R121, *P*-Ahx-NH-NH-MeOHe-R121, *P*-Ahx-R121, *P*-Ahx-NH-N═MeOHe-RIT, or *P*-Ahx-NH-NH-MeOHe-RIT at the indicated concentration of Dox for 72 h under standard culture conditions. Cell proliferation was assessed using [^{3}H]-thymidine incorporation by adding this tracer to the cultures for the last 6 h of incubation. The results are shown as the inhibition of the proliferation of the exposed cells relative to controls (cells incubated in medium only). The activity of the control cells was always greater than 50 000 cpm/well. Each experimental point is the average of three experiments ± SD.

to Dox beginning at 1.5 μM, and approximately 50-fold increase in the sensitization to Dox was achieved at 24 μM (Figure 7A). The conjugates *P*-Ahx-NH-NH-MeOHe-R121 and *P*-Ahx-R121, used as controls, showed no activity. The *P*-Ahx-NH-N═MeOHe-RIT conjugate did not sensitize the cells to Dox at concentrations up to 3 μM. This conjugate showed moderate activity at 6 μM (~10-fold increase in sensitization), and a 50-fold increase in sensitization (comparable to conjugate *P*-Ahx-NH-N═MeOHe-R121 at 24 μM) was observed at 12 μM. However, the *P*-Ahx-NH-N═MeOHe-RIT conjugate showed some toxicity at 12 μM. Therefore, we cannot exclude the possibility that the unexpectedly high sensitization activity observed was due in part to its toxicity (Figure 7B). The *P*-Ahx-NH-NH-MeOHe-RIT conjugate, used as a control, showed no activity.

Cytostatic Activity of the *P*(HPMA) Conjugates *P*-Ahx-NH-N═MeOHe-R121(Dox) and *P*-Ahx-NH-N═MeOHe-RIT(Dox) in Vitro. Finally, the cytostatic activity of the conjugate *P*-Ahx-NH-N═MeOHe-R121(Dox) containing Dox and the P-gp inhibitor MeOHe-R121, both bound via hydrazone bonds to the *P*(HPMA) carrier, was determined and compared to that of the mixture of the two conjugates, *P*-Ahx-NH-N═MeOHe-R121 and *P*-Ahx-NH-N═Dox. The *P*-Ahx-NH-N═MeOHe-R121(Dox) conjugate was far more cytostatic than conjugate *P*-Ahx-NH-N═Dox (Figure 8A), and the calculated IC_{50} was almost 30 times lower. This conjugate was also slightly (less than twice) more cytostatic than the comparable mixture of the conjugates *P*-Ahx-NH-N═MeOHe-R121 and *P*-Ahx-NH-N═Dox.

Polymer conjugate *P*-Ahx-NH-N═MeOHe-RIT(Dox) exerted almost 10 times higher cytostatic activity than *P*-Ahx-NH-N═Dox; however, it had slightly lower cytostatic activity than the mixture of *P*-Ahx-NH-N═MeOHe-RIT and *P*-Ahx-NH-N═Dox (Figure 8B).

Thus, we have demonstrated that simultaneous delivery of cytostatic drug and P-gp inhibitor used either as a mixture of single drug and single inhibitor-bearing *P*(HPMA) conjugates or, better, as a combination of both molecules bound to the same polymer carrier is a promising strategy to overcome multidrug resistance in cancer cells.

■ CONCLUSIONS

The potential for novel polymeric therapeutics based on water-soluble *P*(HPMA) conjugates bearing either the anticancer drug doxorubicin, an inhibitor of ABC transporters or both to increase the efficacy of Dox treatment of the Dox-resistant P-gp-expressing P388/MDR leukemia cells was studied. Several oxoacid analogues of the inhibitors of the ABC transporters reversin 121, reversin 205, and ritonavir oxoacid esters were synthesized, and their ability to inhibit P-gp mediated Dox efflux in P388/MDR cells was evaluated. MeOHe-R121 and MeOHe-RIT retained the inhibitory activity of the parent

dx.doi.org/10.1021/bm500649q | *Biomacromolecules* XXXX, XXX, XXX−XXX

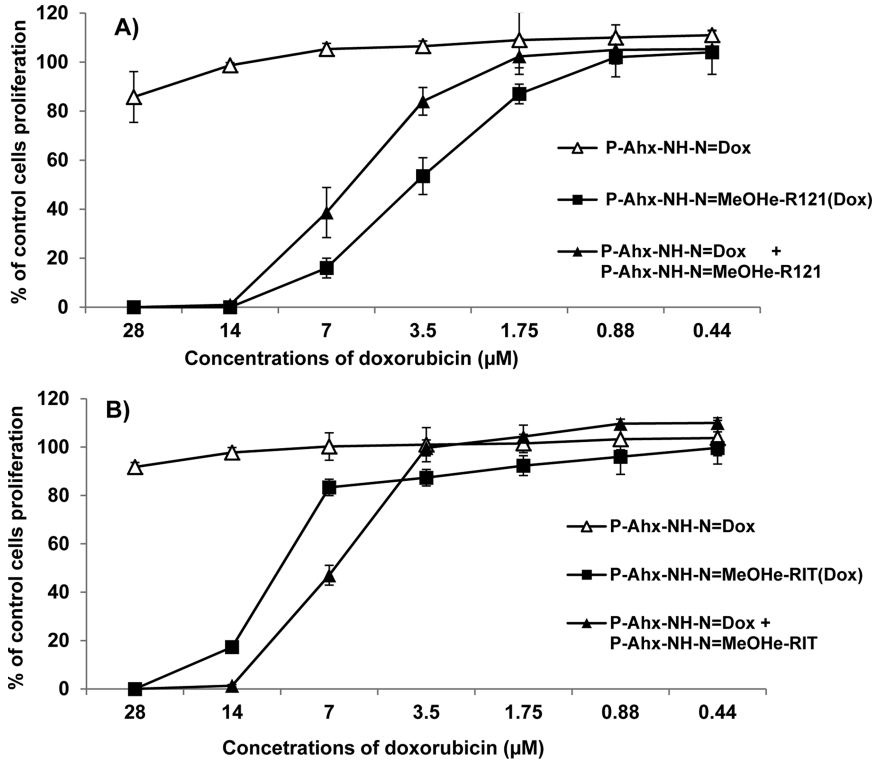

Figure 8. Overcoming multidrug resistance in P388/MDR cells in vitro by simultaneous delivery of the conjugates *P*-Ahx-NH-N═Dox and *P*-Ahx-NH-N═MeOHe-R121 in an equimolar drug/inhibitor ratio, or by the conjugate *P*-Ahx-NH-N═MeOHe-R121(Dox) bearing both Dox and MeOHe-R121 bound via hydrazone bonds (A) or by conjugates *P*-Ahx-NH-N═Dox and *P*-Ahx-NH-N═MeOHe-RIT or *P*-Ahx-NH-N═MeOHe-RIT(Dox) containing Dox and P-gp inhibitor MeOHe-RIT (B). P388/MDR cells were incubated with titrated concentrations of *P*-Ahx-NH-N═Dox, with a mixture of *P*-Ahx-NH-N═Dox and *P*-Ahx-NH-N═MeOHe-R121 or conjugate *P*-Ahx-NH-N═MeOHe-R121(Dox) or with a mixture of *P*-Ahx-NH-N═Dox and *P*-Ahx-NH-N═MeOHe-RIT or conjugate *P*-Ahx-NH-N═MeOHe-RIT(Dox) for 72 h at standard cultivation conditions. The concentration of MeOHe-R121 or MeOHe-RIT was proportional to Dox concentration with the ratio 1:1 throughout the experiment. Cell proliferation was assessed by [^{3}H]-thymidine incorporation which was added to the cultures for the last 6 h of incubation. Results are shown as inhibition of exposed cell proliferation relative to controls (cells incubated in medium only). The activity of control cells was always higher than 50 000 cpm/well. Each experimental point is average of three experiments ± SD.

inhibitors, while MeOHe-R205 showed no P-gp inhibitory activity.

The polymer conjugates *P*-Ahx-NH-N═MeOHe-R121 and *P*-Ahx-NH-N═MeOHe-RIT, in which the MeOHe-R121 and MeOHe-RIT, respectively, were bound to the water-soluble polymer carrier via pH-senzitive hydrazone bonds, were synthesized. *P*-Ahx-NH-N═MeOHe-R121 showed no toxicity up to 24 μM, and only modest toxicity was observed at 48 μM. In contrast, the *P*-Ahx-NH-N═MeOHe-RIT conjugate was significantly toxic at concentrations of 24 and 48 μM, but little or no toxicity was observed at concentrations below 12 μM. Both conjugates, *P*-Ahx-NH-N═MeOHe-R121 and *P*-Ahx-NH-N═MeOHe-RIT, showed very good P-gp inhibitory activity. On the other hand, the conjugates *P*-Ahx-NH-NH-MeOHe-R121, *P*-Ahx-R121, *P*-Ahx-NH-NH-MeOHe-RIT, and *P*-Ahx-RIT, which contained MeOHe-R121, reversin 121, MeOHe-RIT, and ritonavir, respectively, bound to the carrier via nonbiodegradable bonds, showed no toxicity and no P-gp inhibitory activity.

At 24 μM, the *P*-Ahx-NH-N═MeOHe-R121 conjugate increases the sensitivity of the P388/MDR cells to Dox by approximately 50-fold. The *P*-Ahx-NH-N═MeOHe-RIT conjugate showed moderate activity at 6 μM (~10 times higher sensitivity), and at 12 μM this conjugate increased the sensitivity of the P388/MDR to Dox treatment by 50-fold.

The IC_{50} for the *P*-Ahx-NH-N═MeOHe-R121(Dox) conjugate, which contains both Dox and the P-gp inhibitor MeOHe-R121 bound to the same carrier via hydrazone bonds, was almost 30 times lower than that for the *P*-Ahx-NH-N═Dox conjugate. This IC_{50} was less than two times lower than the IC_{50} for the comparable mixture of the two conjugates, *P*-Ahx-NH-N═MeOHe-R121 and *P*-Ahx-NH-N═Dox. Similarly, *P*-Ahx-NH-N═MeOHe-RIT(Dox) containing Dox and MeOHe-RIT as a P-gp inhibitor both bound to the same carrier was almost 10 times more cytostatic than *P*-Ahx-NH-N═Dox. Contrary to the case of *P*-Ahx-NH-N═MeOHe-R121(Dox), the cytostatic activity of *P*-Ahx-NH-N═MeOHe-RIT(Dox) was slightly less cytostatic than the mixture of conjugates *P*-Ahx-NH-N═MeOHe-RIT and *P*-Ahx-NH-N═Dox.

These results have confirmed that the use of water-soluble *P*(HPMA) conjugates used to deliver a cytostatic drug and a P-gp inhibitor simultaneously represents a promising strategy to overcome multidrug resistance in cancer cells.

■ ASSOCIATED CONTENT

Ⓢ Supporting Information

^{1}H NMR spectra of the synthesized compounds. Tables containing the IC_{50} values determined in sensitive P388 and multidrug-resistant P388/MDR cell lines for Dox and *P*(HPMA) conjugate *P*-Ahx-NHN═Dox and IC_{50} values determined in multidrug-resistant P388/MDR cell line for

dx.doi.org/10.1021/bm500649q | *Biomacromolecules* XXXX, XXX, XXX−XXX

doxorubicin in the presence of different P-gp inhibitors. This material is available free of charge via the Internet at http://pubs.acs.org.

AUTHOR INFORMATION

Corresponding Author

*Tel.: +420-296809389. Fax: +420-296809410. E-mail: subr@imc.cas.cz.

Notes

The authors declare no competing financial interest.

ACKNOWLEDGMENTS

The work was supported by the Grant Agency of the Czech Republic (Grant No. P301/12/1254) and by the project BIOCEV - Biotechnology and Biomedicine Centre of the Academy of Sciences and Charles University (CZ.1.05/1.1.00/02.0109) from the European Regional Development Fund. The authors appreciate the excellent technical assistance of Helena Mišurcová and Pavlína Jungrová.

REFERENCES

(1) Gottesman, M. M. *Cancer Res.* **1993**, *53*, 747−754.
(2) Nobili, S.; Landini, I.; Mazzei, T.; Mini, E. *Med. Res. Rev.* **2012**, *32*, 1220−1262.
(3) Gottesman, M. M.; Pastan, I. *Annu. Rev. Biochem.* **1993**, *62*, 385−427.
(4) Tiwari, A. K.; Sodani, K.; Dai, C. L.; Ashby, C. R.; Chen, Z. S.; Chen, Z. S. *Curr. Pharm. Biotechnol.* **2011**, *12*, 570−594.
(5) Szakács, G.; Váradi, A.; Özvegy-Laczka, C.; Sarkadi, B. *Drug Discovery Today* **2008**, *13*, 379−393.
(6) Schinkel, A. H.; Jonker, J. W. *Adv. Drug Delivery Rev.* **2012**, *64* (Supplement), 138−153.
(7) Binkhathlan, Z.; Lavasanifar, A. *Current Cancer Drug Targets* **2013**, *13*, 326−346.
(8) Falasca, M.; Linton, K. J. *Expert Opin. Invest. Drugs* **2012**, *21*, 657−666.
(9) Sarkadi, B.; Seprödi, J.; Csuka, O.; Magocsi, M.; Mezo, I.; Teplan, I.; Vadasz, Z.; Vincze, B.; Palyi, I. *Compounds for reversing drug resistance*. 94915684.8, 1994.
(10) Sharom, F. J.; Yu, X. H.; Lu, P. H.; Liu, R. H.; Chu, J. W. K.; Szabo, K.; Muller, M.; Hose, C. D.; Monks, A.; Varadi, A.; Seprodi, J.; Sarkadi, B. *Biochem. Pharmacol.* **1999**, *58*, 571−586.
(11) Yabuki, N.; Sakata, K.; Yamasaki, T.; Terashima, H.; Mio, T.; Miyazaki, Y.; Fujii, T.; Kitada, K. *Cancer Genet. Cytogenet.* **2007**, *173*, 1−9.
(12) Hoffmann, K.; Bekeredjian, R.; Schmidt, J.; Buchler, M. W.; Marten, A. *Tumor Biol.* **2008**, *29*, 351−358.
(13) Koubeissi, A.; Raad, I.; Ettouati, L.; Guilet, D.; Dumontet, C.; Paris, J. *Bioorg. Med. Chem. Lett.* **2006**, *16*, 5700−5703.
(14) Arnaud, O.; Koubeissi, A.; Ettouati, L.; Terreux, R.; Alame, G.; Grenot, C.; Dumontet, C.; Di Pietro, A.; Paris, J.; Falson, P. *J. Med. Chem.* **2010**, *53*, 6720−6729.
(15) Omelyanenko, V.; Kopečková, P.; Gentry, C.; Kopeček, J. *J. Controlled Release* **1998**, *53*, 25−37.
(16) Kunjachan, S.; Blauz, A.; Möckel, D.; Theek, B.; Kiessling, F.; Etrych, T.; Ulbrich, K.; Bloois, L. V.; Storm, G.; Bartosz, G.; Rychlik, B.; Lammers, T. *Eur. J. Pharm. Sci.* **2012**, *45*, 421−428.
(17) Kopeček, J. *Adv. Drug Delivery Rev.* **2013**, *65*, 49−59.
(18) Alakhova, D. Y.; Rapoport, N. Y.; Batrakova, E. V.; Timoshin, A. A.; Li, S.; Nicholls, D.; Alakhov, V. Y.; Kabanov, A. V. *J. Controlled Release* **2010**, *142*, 89−100.
(19) Alakhov, V. Y.; Moskaleva, E. Y.; Batrakova, E. V.; Kabanov, A. V. *Bioconjugate Chem.* **1996**, *7*, 209−216.
(20) Xiao, L.; Xiong, X.; Sun, X.; Zhu, Y.; Yang, H.; Chen, H.; Gan, L.; Xu, H.; Yang, X. *Biomaterials* **2011**, *32*, 5148−5157.
(21) Zhang, X.; Guo, S.; Fan, R.; Yu, M.; Li, F.; Zhu, C.; Gan, Y. *Biomaterials* **2012**, *33*, 7103−7114.
(22) Zhao, Y. Z.; Dai, D. D.; Lu, C. T.; Chen, L. J.; Lin, M.; Shen, X. T.; Li, X. K.; Zhang, M.; Jiang, X.; Jin, R. R.; Li, X.; Lv, H. F.; Cai, L.; Huang, P. T. *Cancer Lett.* **2013**, *330*, 74−83.
(23) Prasad, P.; Cheng, J.; Shuhendler, A.; Rauth, A. M.; Wu, X. Y. *Drug Delivery Transl. Res.* **2012**, *2*, 95−105.
(24) Shalviri, A.; Raval, G.; Prasad, P.; Chan, C.; Liu, Q.; Heerklotz, H.; Rauth, A. M.; Wu, X. Y. *Eur. J. Pharm. Biopharm.* **2012**, *82*, 587−597.
(25) Hu, C. M. J.; Zhang, L. *Biochem. Pharmacol.* **2012**, *83*, 1104−1111.
(26) Minko, T.; Kopečková, P.; Kopeček, J. *J. Controlled Release* **1999**, *59*, 133−148.
(27) Minko, T.; Kopečková, P.; Pozharov, V.; Kopeček, J. *J. Controlled Release* **1998**, *54*, 223−233.
(28) Minko, T.; Kopečková, P.; Kopeček, J. *Macromol. Symp.* **2001**, *172*, 35−47.
(29) Minko, T. *Adv. Drug Delivery Rev.* **2010**, *62*, 192−202.
(30) Šťastný, M.; Plocová, D.; Etrych, T.; Ulbrich, K.; Říhová, B. *Eur. J. Cancer* **2002**, *38*, 602−608.
(31) Batrakova, E. V.; Li, S.; Brynskikh, A. M.; Sharma, A. K.; Li, Y. L.; Boska, M.; Gong, N.; Mosley, R. L.; Alakhov, V. Y.; Gendelman, H. E.; Kabanov, A. V. *J. Controlled Release* **2010**, *143*, 290−301.
(32) Maeda, H.; Nakamura, H.; Fang, J. *Adv. Drug Delivery Rev.* **2013**, *65*, 71−79.
(33) Chytil, P.; Etrych, T.; Kříž, J.; Šubr, V.; Ulbrich, K. *Eur. J. Pharm. Sci.* **2010**, *41*, 473−482.
(34) Drobník, J.; Kopeček, J.; Labský, J.; Rejmanová, P.; Exner, J.; Saudek, V.; Kálal, J. *Makromol. Chem.* **1976**, *177*, 2833−2848.
(35) Šubr, V.; Ulbrich, K. *React. Funct. Polym.* **2006**, *66*, 1525−1538.
(36) Barberis, M.; Pérez-Prieto, J. *Tetrahedron Lett.* **2003**, *44*, 6683−6685.
(37) Peters, C.; Waldmann, H. *J. Org. Chem.* **2003**, *68*, 6053−6055.
(38) Perrier, S.; Takolpuckdee, P.; Mars, C. A. *Macromolecules* **2005**, *38*, 2033−2036.
(39) Etrych, T.; Mrkvan, T.; Chytil, P.; Koňák, Č.; Říhová, B.; Ulbrich, K. *J. Appl. Polym. Sci.* **2008**, *109*, 3050−3061.
(40) Etrych, T.; Jelínková, M.; Říhová, B.; Ulbrich, K. *J. Controlled Release* **2001**, *73*, 89−102.
(41) Arnaud, O.; Koubeissi, A.; Ettouati, L.; Terreux, R.; Alame, G.; Grenot, C.; Dumontet, C.; Di Pietro, A.; Paris, J.; Falson, P. *J. Med. Chem.* **2010**, *53*, 6720−6729.
(42) Etrych, T.; Šírová, M.; Starovoytova, L.; Říhová, B.; Ulbrich, K. *Mol. Pharmaceutics* **2010**, *7*, 1015−1026.
(43) Kostková, H.; Říhová, B.; Etrych, T.; Ulbrich, K. *J. Bioact. Compat. Polym.* **2011**, *26*, 270−286.
(44) Kostková, H.; Etrych, T.; Říhová, B.; Kostka, L.; Starovoytova, L.; Kovář, M.; Ulbrich, K. *Macromol. Biosci.* **2013**, *13*, 1648−1660.
(45) Sadzuka, Y.; Egawa, Y.; Sawanishi, H.; Miyamoto, K.; Sonobe, T. *Toxicol. Lett.* **2002**, *135*, 137−144.

Supporting informations

Synthesis of Poly[*N*-(2-hydroxypropyl)methacrylamide] Conjugates with Inhibitors of ABC Transporter That Overcome Multidrug Resistance in Doxorubicin-Resistant P388 cells in vitro

V.Šubr[1*], L.Sivák[2], E.Koziolová[1], A.Braunová[1], M.Pechar[1], J.Strohalm[1], M.Kabešová[2], B.Říhová[2], K.Ulbrich[1], M.Kovář[2]

[1] *Institute of Macromolecular Chemistry, Academy of Sciences of the Czech Republic v.v.i., Heyrovsky Sq. 2, 162 06 Prague 6, Czech Republic*

[2] *Institute of Microbiology, Academy of Sciences of the Czech Republic v.v.i., Vídeňská 1083, 142 20 Prague 4, Czech Republic*

*corresponding author: subr@imc.cas.cz

Table of content:

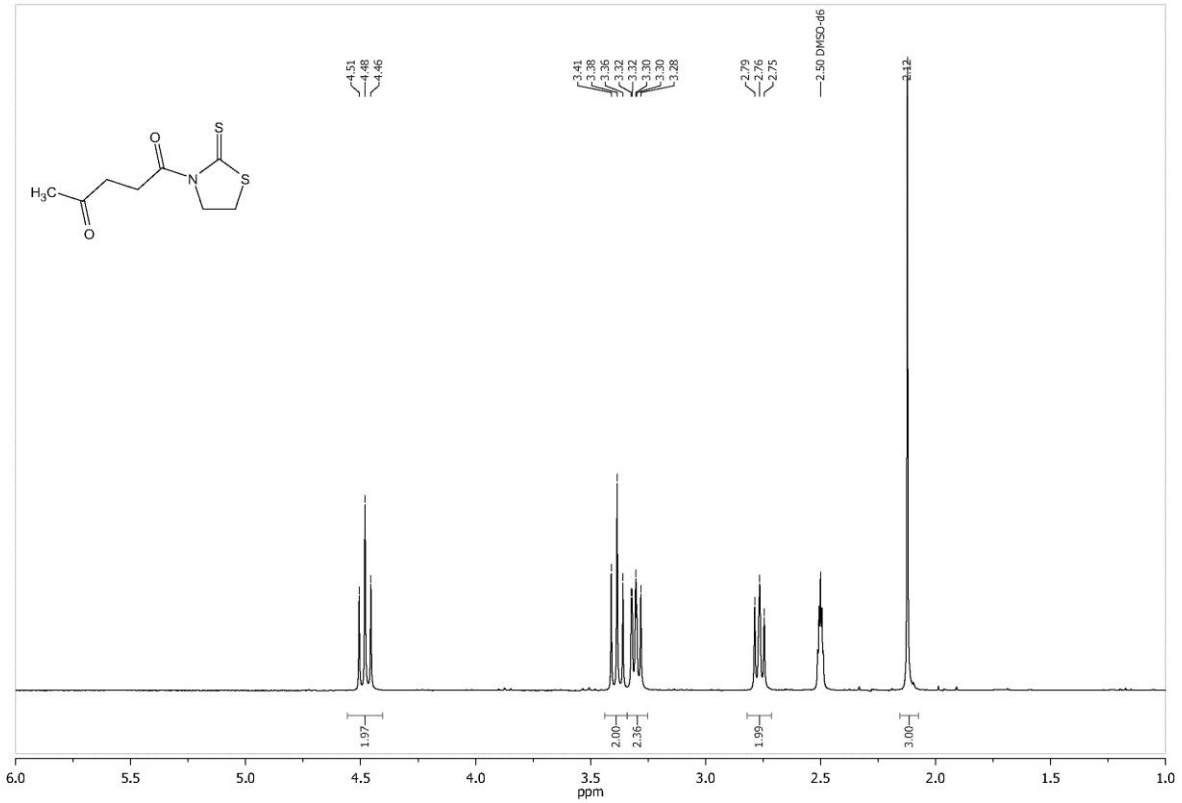

Figure S1 ^{1}H NMR spectrum (300 MHz; DMSO; 296 K) of 1-(2-thioxo-thiazolidin-3-yl)-pentane-1,4-dione (OPe-TT)

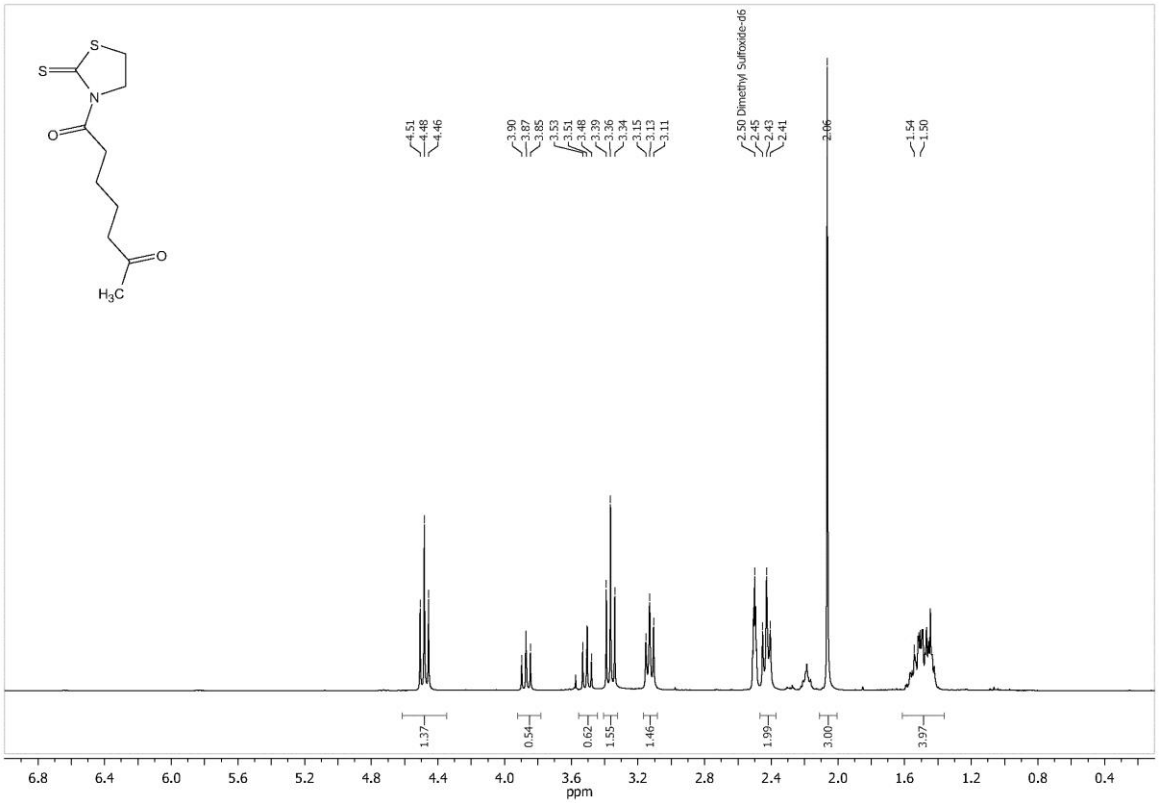

Figure S2 ^{1}H NMR spectrum (300 MHz; DMSO; 296 K) of 1-(2-thioxo-thiazolidin-3-yl)-heptane-1,6-dione (OHe-TT)

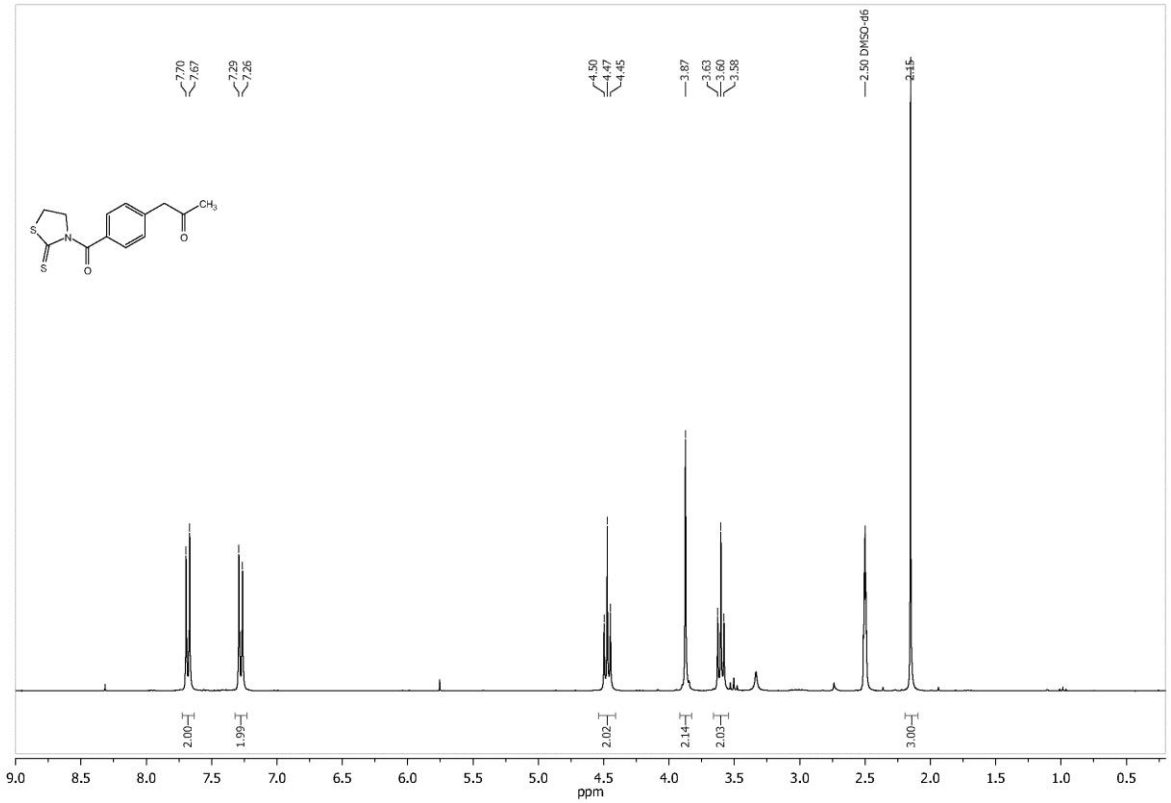

Figure S3 ^{1}H NMR spectrum (300 MHz; DMSO; 296 K) of 1-[4-(2-thioxo-thiazolidine-3-carbonyl)-phenyl]-propan-2-one (OPB-TT)

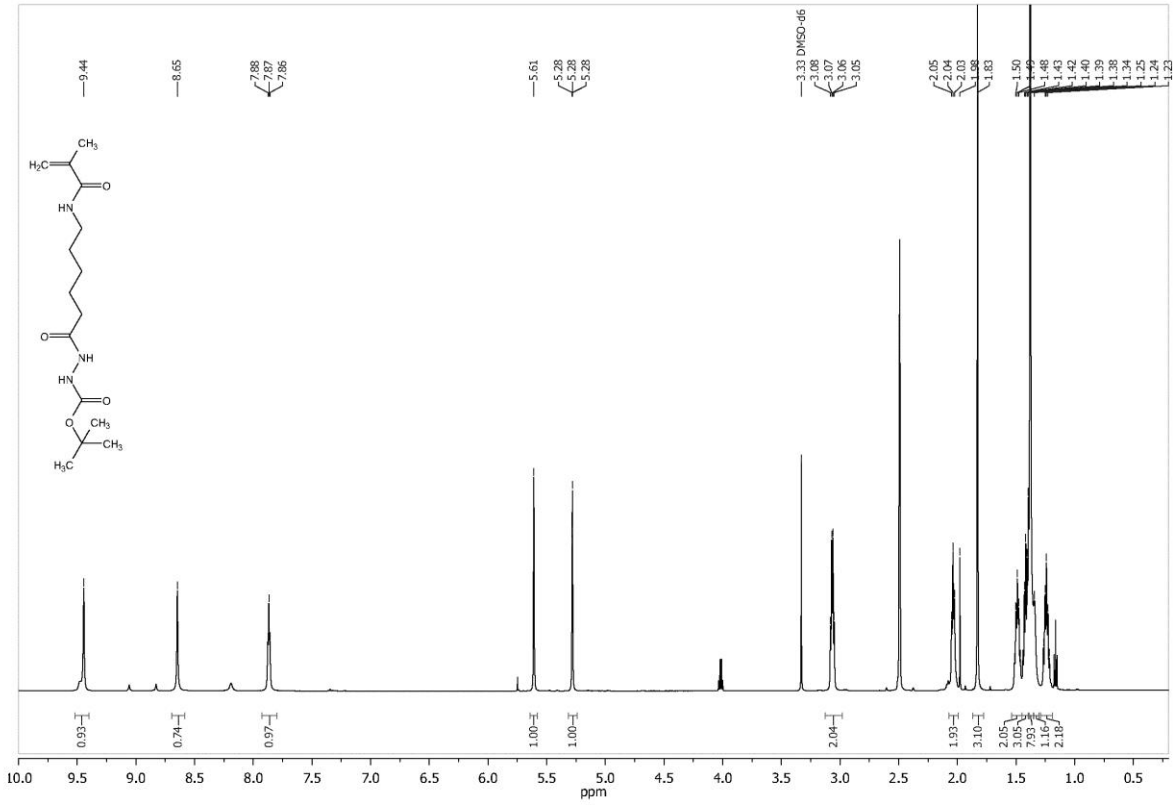

Figure S4 ^{1}H NMR spectrum (300 MHz; DMSO; 296 K) of *N*'-[6-(2-Methyl-acryloylamino)-hexanoyl]-hydrazinecarboxylic acid tert-butyl ester (Ma-Ahx-NH-NH-Boc)

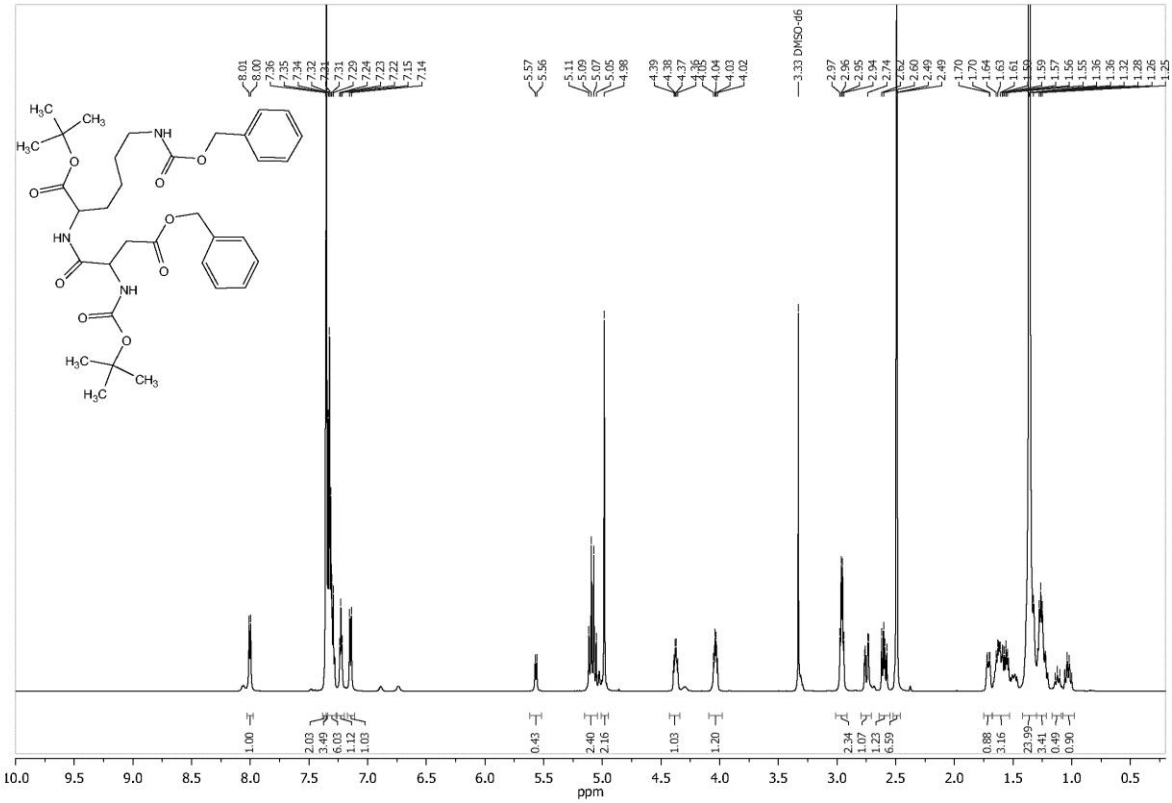

Figure S5 ^{1}H NMR spectrum (300 MHz; DMSO; 296 K) of Boc-Asp(OBzl)-Lys(Z)-OtBu, (Reversin 121)

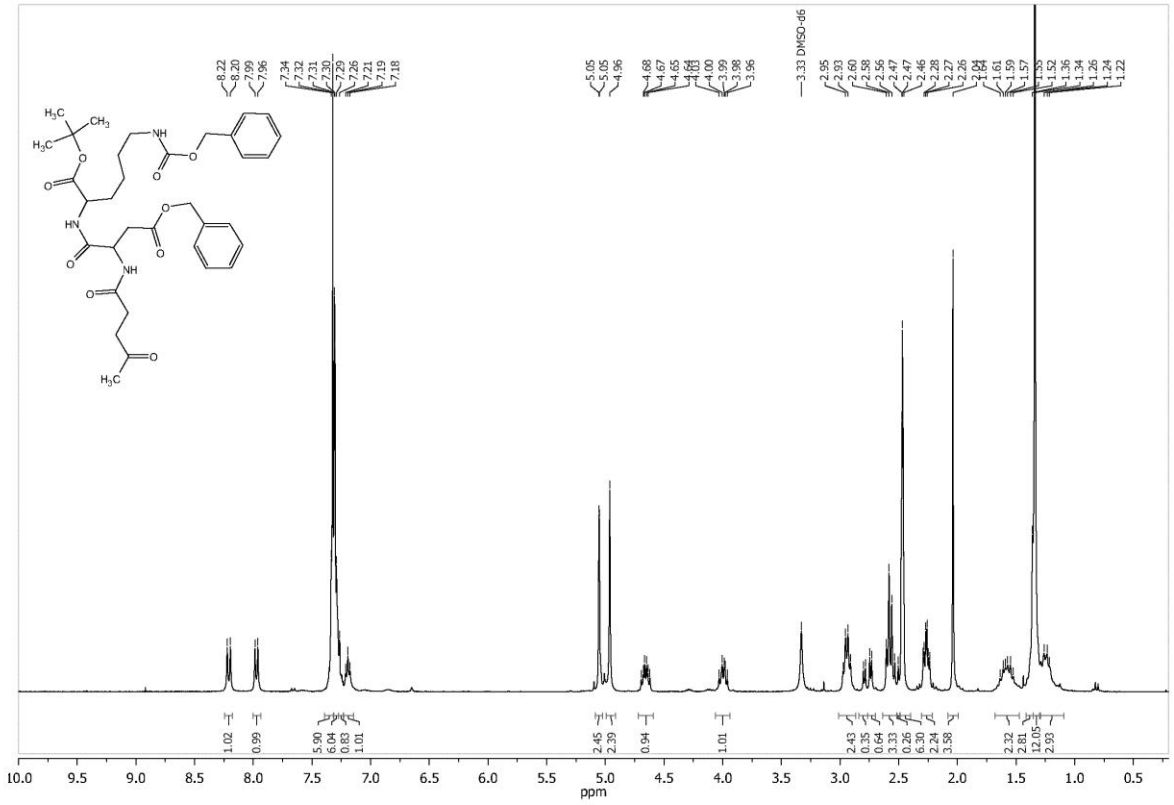

Figure S6 ^{1}H NMR spectrum (300 MHz; DMSO; 296 K) of OPe-Asp(OBzl)-Lys(Z)-OtBu, (OPe-R121)

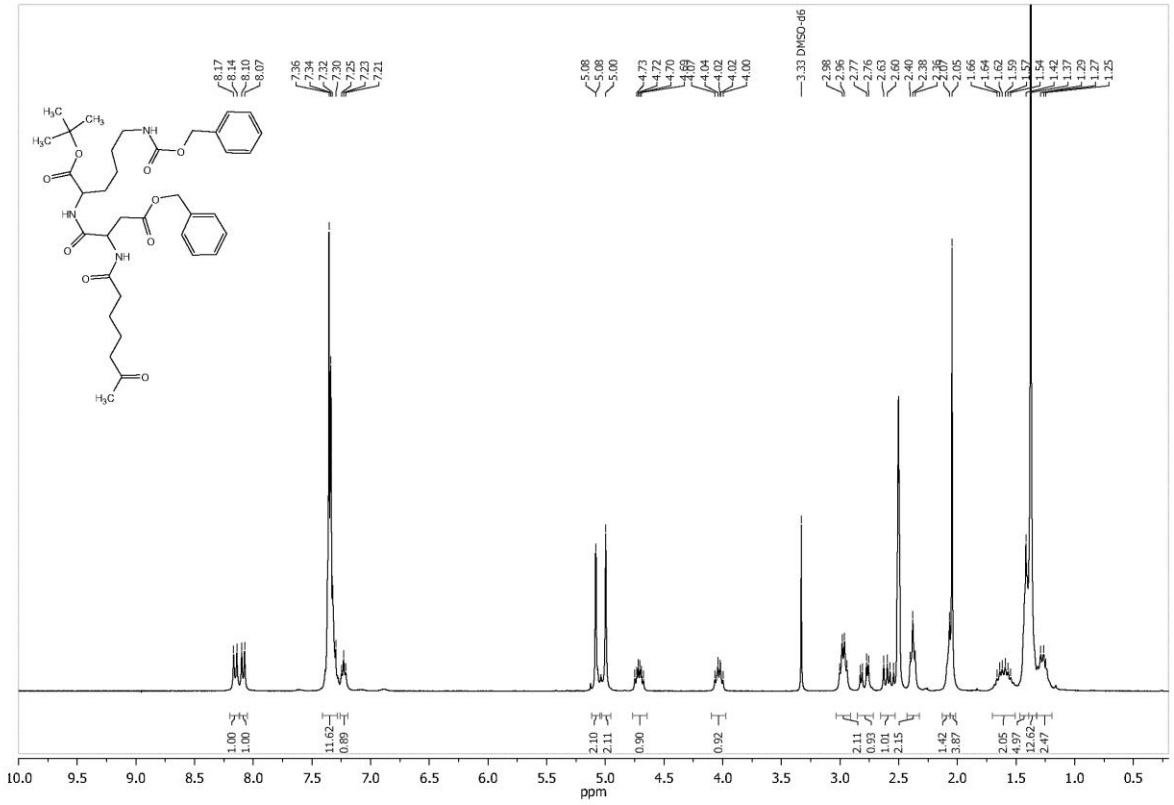

Figure S7 ^{1}H NMR spectrum (300 MHz; DMSO; 296 K) of OHe-Asp(OBzl)-Lys(Z)-OtBu, (OHe-R121)

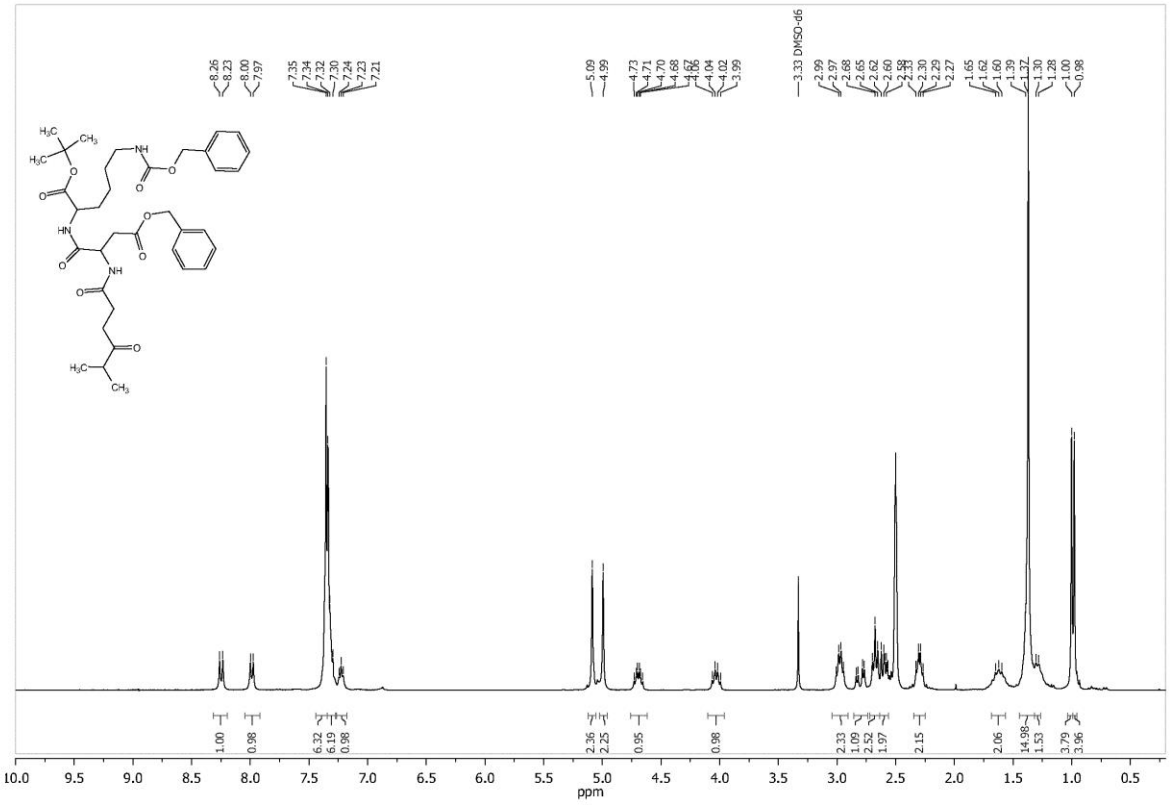

Figure S8 ^{1}H NMR spectrum (300 MHz; DMSO; 296 K) of MeOHe-Asp(OBzl)-Lys(Z)-OtBu, (MeOHe-R121)

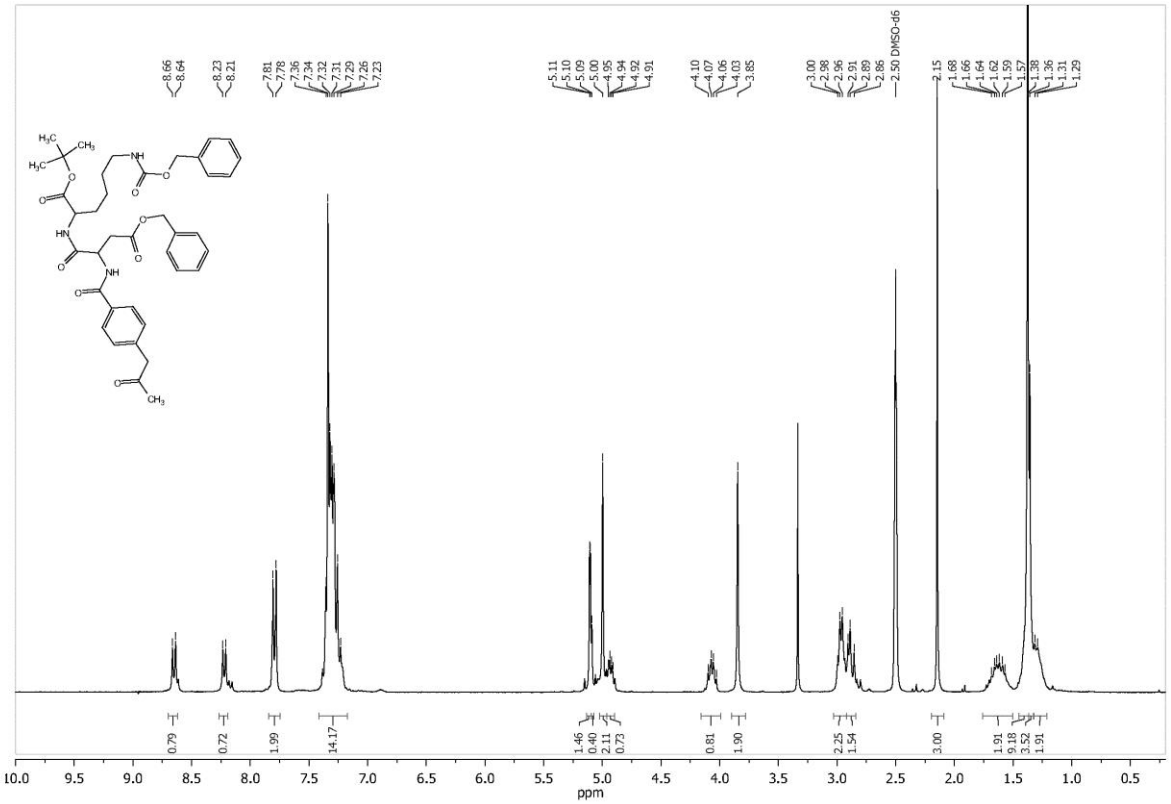

Figure S9 ^{1}H NMR spectrum (300 MHz; DMSO; 296 K) of OPB-Asp(OBzl)-Lys(Z)-OtBu, (OPB-R121)

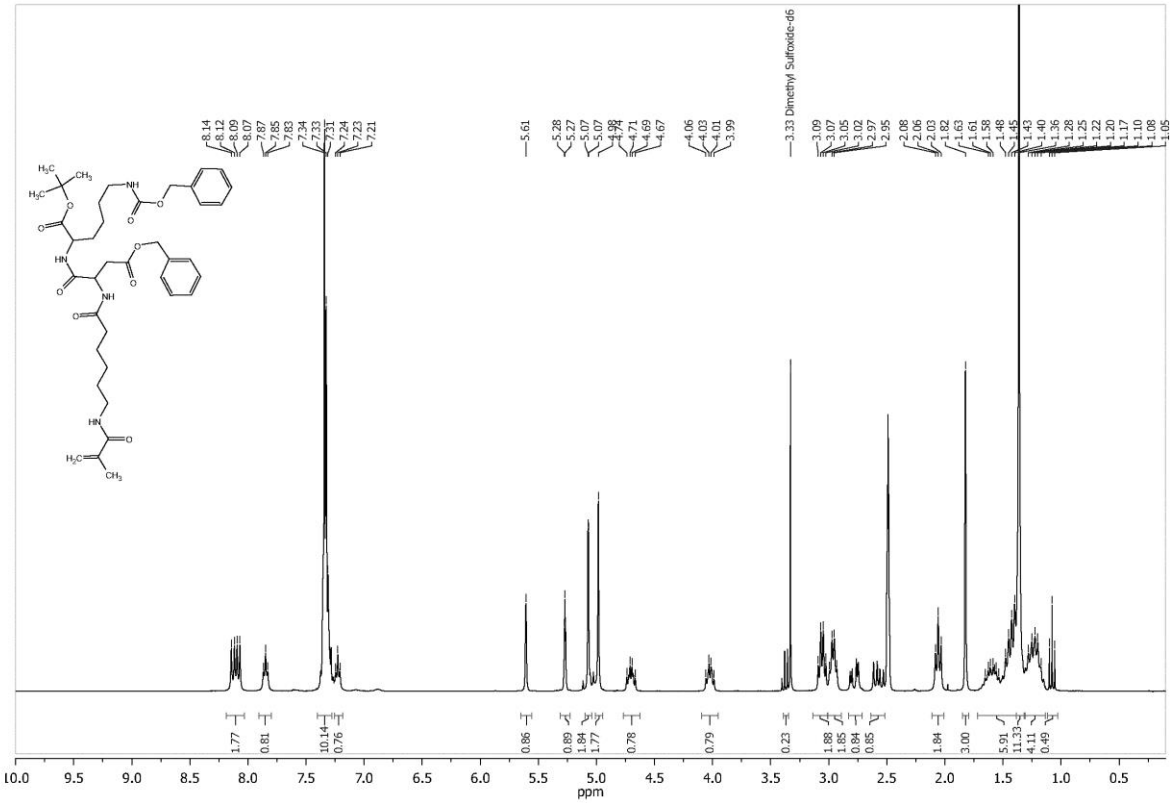

Figure S10 ^{1}H NMR spectrum (300 MHz; DMSO; 296 K) of 6-(2-methyl-acryloylamino)-hexanoyl-Asp(OBzl)-Lys(Z)-OtBu (Ma-Ahx-R121)

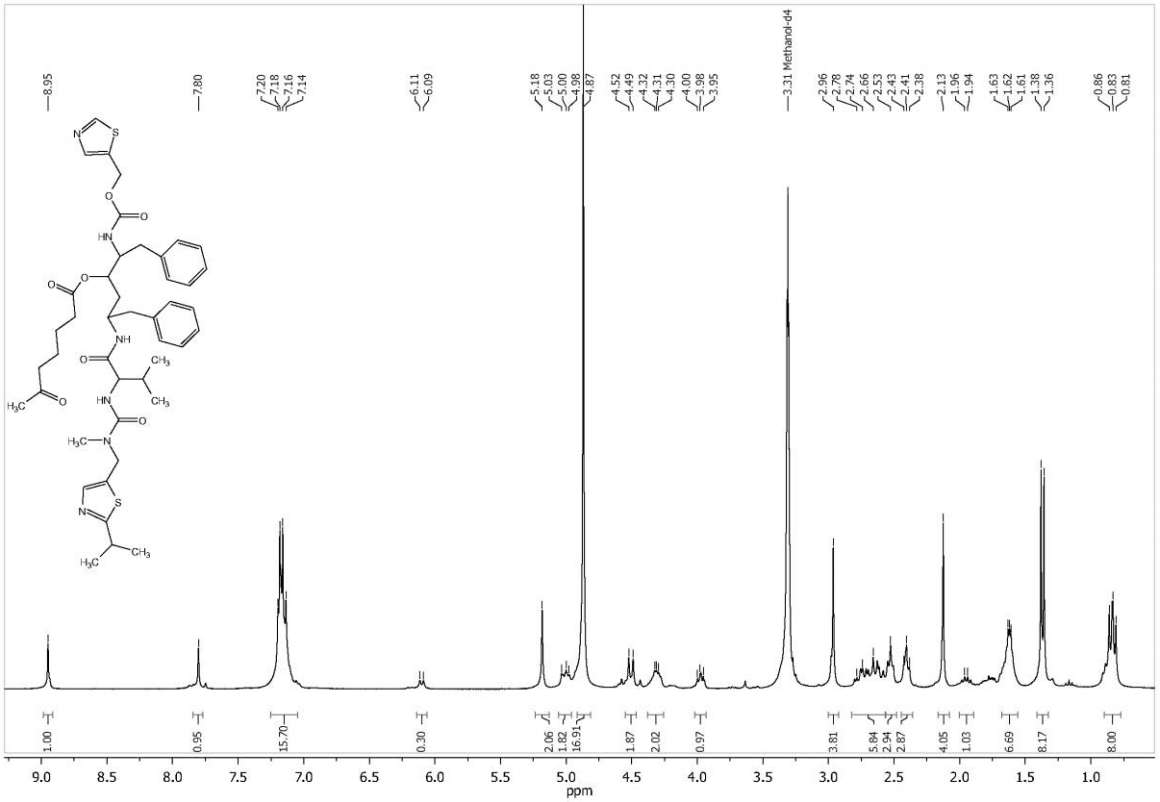

Figure S11 ^{1}H NMR spectrum (300 MHz; methanol; 296 K) of 6-oxoheptanoyl-ritonavir ester (OHe-RIT)

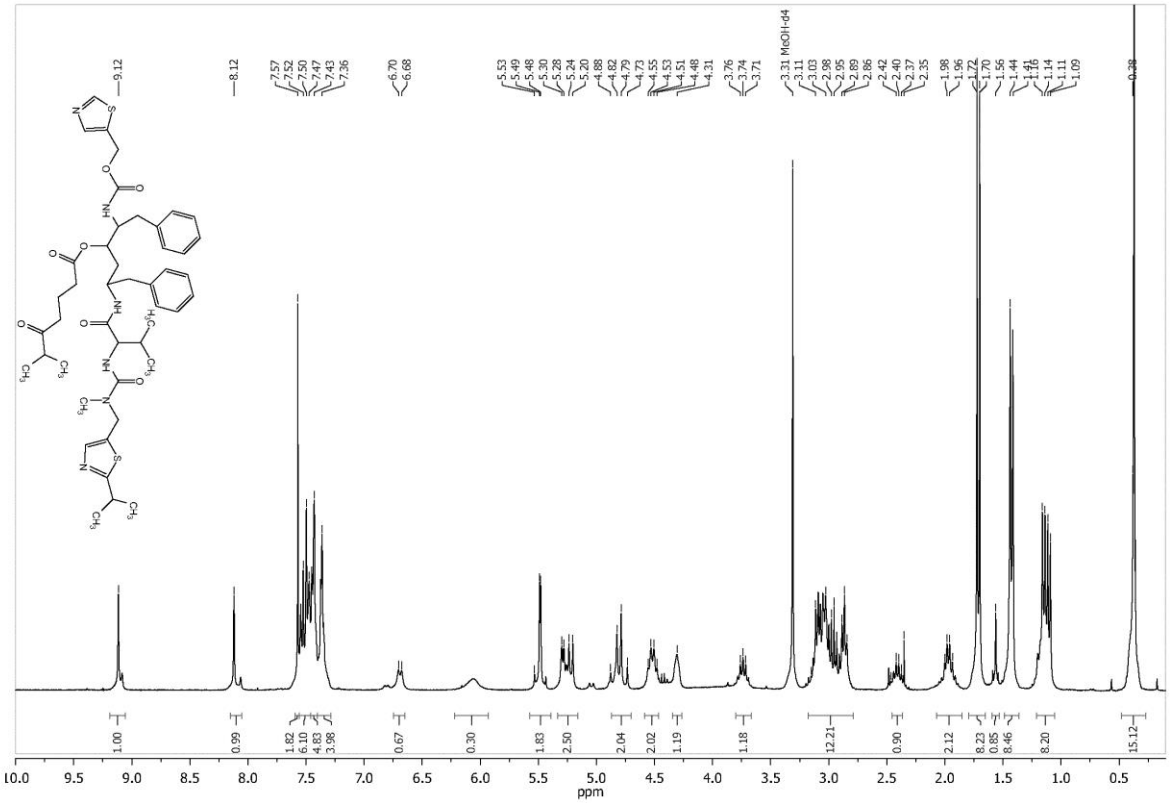

Figure S12 ^{1}H NMR spectrum (300 MHz; methanol; 296 K) 5-methyl-4-oxohexanoyl-ritonavir ester (MeOHe-RIT)

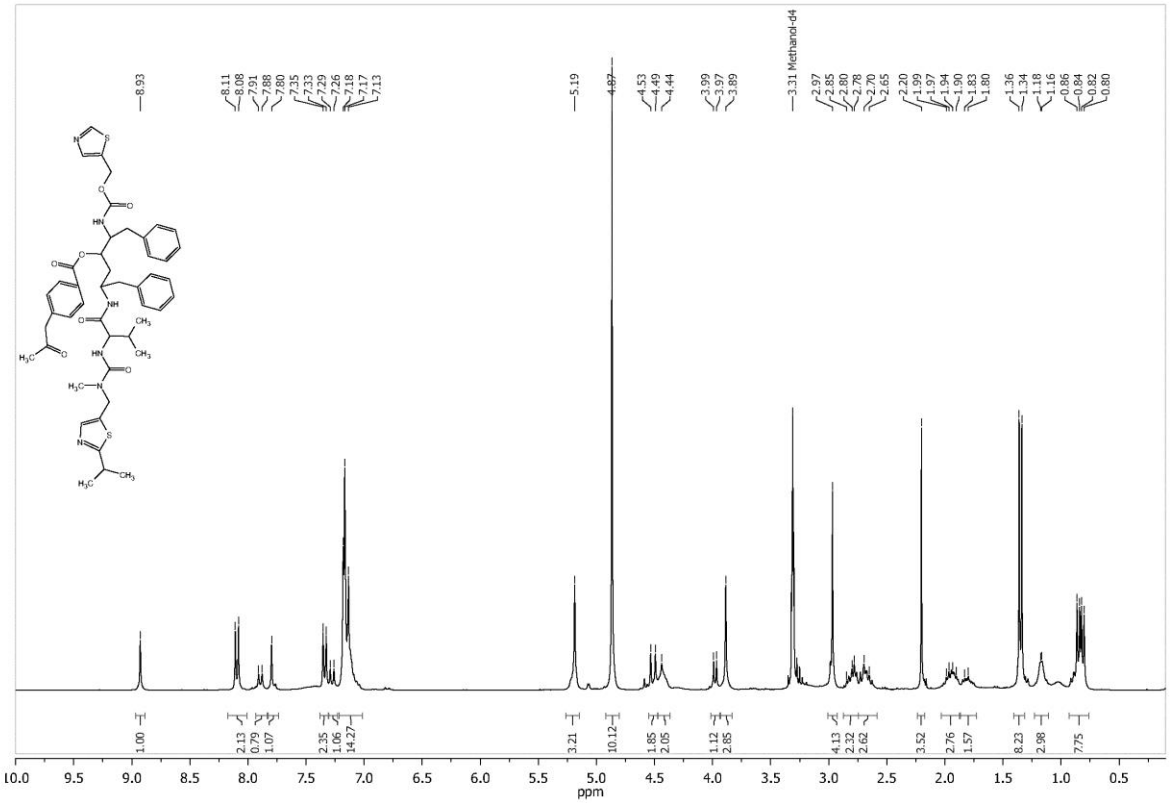

Figure S13 ^{1}H NMR spectrum (300 MHz; methanol; 296 K) of 4-(2-oxopropyl)-benzoyl-ritonavir ester (OPB-RIT)

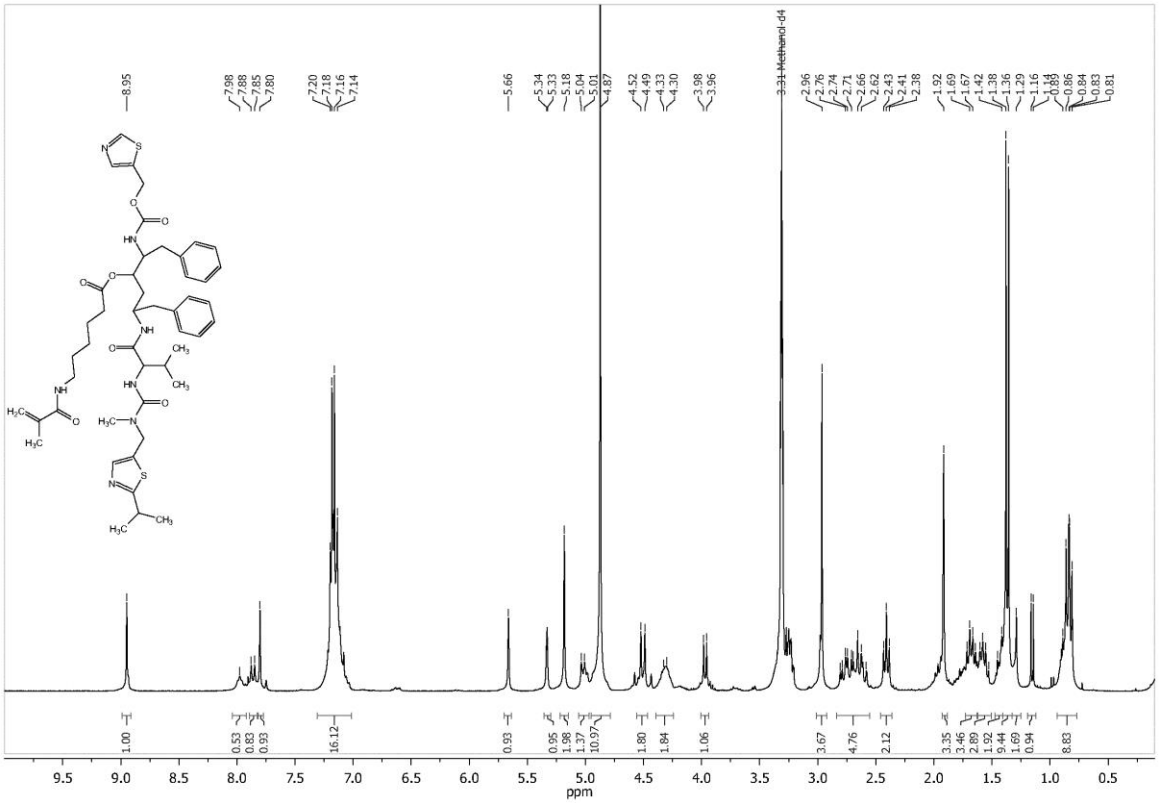

Figure S14 ^{1}H NMR spectrum (300 MHz; methanol; 296 K) of 6-(2-methyl-acryloylamino)-hexanoyl-ritonavir ester (Ma-Ahx-RIT)

Supplementary Table 1. IC_{50} values determined in sensitive P388 and multidrug resistant P388/MDR cell lines for Dox and *P*(HPMA) conjugate *P*-Ahx-NHN=Dox.

Type of drug	**P388 IC_{50} (μM)[a]**	**P388/MDR IC_{50} (μM)**	**Resistance ratio**
Dox	0.0098 ± 0.001	5.86 ± 0.41	598
P-Ahx-NHN=Dox	0.024 ± 0.001	91.7 ± 11.8	3821

[a] IC_{50} (μM) values were calculated as concentration of doxorubicin which inhibits after 72 hours of cultivation (see Materials and Methods) the incorporation of [^{3}H]-thymidine by exposed cells to 50 % of the controls. The activity of control cells was always higher than 50 000 cpm/well. Experiments were repeated 5-9 times and average value ± SE is shown. The resistance ratio was calculated by dividing the IC_{50} value for P-388-MDR cell line by corresponding value in P-388 cells. Dox: doxorubicin; P-Ahx-NHN=Dox: HPMA copolymer-bound Dox.

Supplementary Table 2. IC_{50} values determined in multidrug resistant P388/MDR cell line for doxorubicin in presence of different P-gp inhibitors.[a]

	Type of inhibitor				
	Reversin 121	OPe-R121	OHe-R121	MeOHe-R121	OPB-R121
Dox + inhibitor 4 μM	< 0.20	1.09 ± 0.52	0.93 ± 0.21	< 0.10	0.59 ± 0.38
Dox + inhibitor 2 μM	0.24 ± 0.01	3.14 ± 1.81	2.33 ± 0.45	0.17 ± 0.01	1.88 ± 0.86
Dox + inhibitor 1 μM	0.43 ± 0.05	4.88 ± 1.71	3.86 ± 0.47	0.39 ± 0.10	5.10 ± 1.29
Dox + inhibitor 0.5 μM	0.72 ± 0.03	6.69 ± 3.65	4.21 ± 1.12	1.17 ± 0.22	6.53 ± 1.71

[a] IC_{50} (μM) values were calculated as concentration of doxorubicin which inhibits after 72 hours of cultivation (see Materials and Methods) the incorporation of [^{3}H]-thymidine by exposed cells to 50 % of the controls. The activity of control cells was always higher than 50 000 cpm/well. Experiments were repeated 5-9 times and average value ± SE is shown.

Supplementary Table 3. IC_{50} values determined in multidrug resistant P388/MDR cell line for doxorubicin in presence of different P-gp inhibitors.[a]

	Type of inhibitor	
	Reversin 205	MeOHe-R205
Dox + inhibitor 4 μM	0.24 ± 0.03	5.86 ± 0.34
Dox + inhibitor 2 μM	0.47 ± 0.05	5.00 ± 0.34
Dox + inhibitor 1 μM	0.62 ± 0.03	4.74 ± 0.60
Dox + inhibitor 0.5 μM	1.03 ± 0.03	5.94 ± 1.12

[a] IC_{50} (μM) values were calculated as concentration of doxorubicin which inhibits after 72 hours of cultivation (see Materials and Methods) the incorporation of [^{3}H]-thymidine by exposed cells to 50 % of the controls. The activity of control cells was always higher than 50 000 cpm/well. Experiments were repeated 5-9 times and average value ± SE is shown.

Supplementary Table 4. IC_{50} values determined in multidrug resistant P388/MDR cell line for doxorubicin in presence of different P-gp inhibitors.[a]

	Type of inhibitor			
	Ritonavir	OHe-RIT	MeOHe-RIT	OPB-RIT
Dox + inhibitor 10 μM	2.53 ± 0.47	< 0.20	< 0.20	< 0.20
Dox + inhibitor 5 μM	4.34 ± 0.78	2.83 ± 1.00	0.27 ± 0.07	1.72 ± 0.69
Dox + inhibitor 2.5 μM	5.21 ± 0.64	4.36 ± 1.52	2.81 ± 0.40	3.71 ± 0.43
Dox + inhibitor 1.25 μM	5.81 ± 0.74	5.81 ± 1.26	3.62 ± 0.86	4.48 ± 0.86

[a] IC_{50} (μM) values were calculated as concentration of doxorubicin which inhibits after 72 hours of cultivation (see Materials and Methods) the incorporation of [^{3}H]-thymidine by exposed cells to 50 % of the controls. The activity of control cells was always higher than 50 000 cpm/well. Experiments were repeated 5-9 times and average value ± SE is shown.